THE DEVELOPMENT OF ION REGULATION IN EMBRYONIC RAINBOW TROUT, *Oncorhynchus mykiss.*

THE DEVELOPMENT OF ION REGULATION IN EMBRYONIC RAINBOW TROUT, *Oncorhynchus mykiss.*

By

KIMBERLEY J. BARRETT, B.Sc.

A Thesis

Submitted to the School of Graduate Studies

in Partial Fulfillment of the Requirements

for the Degree

Master of Science

McMaster University
Hamilton, Ontario

MASTER OF SCIENCE (1998) McMaster University
(Biology) Hamilton, Ontario

TITLE: The Development of Ion Regulation in Embryonic Rainbow Trout, *Oncorhynchus mykiss*.

AUTHOR: Kimberley J. Barrett, B.Sc. (Queen's University)

SUPERVISORS: Dr. M.J. O'Donnell; Dr. D.G. McDonald

NUMBER OF PAGES: ix, 117

ABSTRACT

This study investigated the regulation of Na^+, Ca^{2+}, and Cl^- during development in embryonic rainbow trout (*Oncorhynchus* mykiss). Because there is a close relationship between pH regulation and ion uptake mechanisms in adult teleosts, pH, pCO_2, and NH_4^+ levels in unstirred layers (USLs) adjacent to whole eggs and dechorionated embryos were determined using double-barrel ion-selective microelectrodes (ISMEs).

Whole eggs accumulated Na^+, Ca^{2+} and Cl^- during the last 20 days of embryonic development, suggesting an ionoregulatory ability prior to hatching.

Na^+ uptake by whole eggs was linearly related to external [Na^+], suggesting that Na^+ crosses the chorion by diffusion. The uptake by dechorionated embryos was saturable, indicating the presence of active transport or facilitated diffusion mechanisms on the surface of embryos prior to hatching.

Ca^{2+} uptake by whole eggs and dechorionated embryos was saturable, suggesting that specific pathways or binding sites are present in the chorion, and that active transport or facilitated diffusion mechanisms are present at the surface of embryos. The much higher J_{max} for whole eggs than dechorionated embryos suggests a role of the perivitelline fluid (pvf) or chorion in ion uptake. J_{max} was lower in dechorionated embryos than in hatchlings suggesting that Ca^{2+} uptake mechanisms may not be fully developed in dechorionated embryos.

Low pH and high [NH_4^+] were measured in the USLs adjacent to whole eggs and dechorionated embryos, relative to the bulk water. A high P_{CO2} measured adjacent to the gills suggests that CO_2 excretion was the primary source of USL acidification. pH was lower in the USL adjacent to the gills and trunk than in the USL adjacent to the yolk sac. [NH_4^+] was highest adjacent to the gills and trunk than adjacent to the yolk sac.

There was no change in the extent of USL acidification or in [NH_4^+] over the last half of embryonic development. After hatching, however, there was a significant increase in [NH_4^+] adjacent to the gills, which was not accompanied by a change in USL pH. It is possible that a change in permeability of the transporting surfaces (i.e. gills, trunk, yolk sac) occurs after hatching.

ACKNOWLEDGEMENTS

I wish to thank Dr. M.J. O'Donnell and Dr. D.G. McDonald for their continuous support, patience, and cooperation during the last two years. I would also like to thank Dr. C.M. Wood for his valuable contribution to the final draft of my thesis.

To all the grad students and post docs from Labs 524, 202, and 203 who have helped me along the way: your friendship and support will never be forgotten.

Finally, I wish to thank my family and my teachers who have influenced me throughout my life. Without your advice and support I may never have travelled this road.

TABLE OF CONTENTS

LIST OF TABLES

Chapter 2:

LIST OF FIGURES

CHAPTER 1: GENERAL INTRODUCTION

Ion Regulation

Challenges of Freshwater Fish

Freshwater fish are hyperosmotic relative to the external water and thus have the tendency to gain water across their gills and lose salts across their gills and kidneys. Freshwater teleosts, such as salmonids, have evolved compensatory ionoregulatory and excretory mechanisms. To maintain water balance, copious amounts of dilute urine are excreted. Solute content is maintained by taking food into the gut and actively taking up ions across specialized cells in the gills (Schmidt-Neilsen, 1994). Ion and osmoregulatory processes in adult teleosts thus require a fully developed gut, branchial, and renal complex.

Although faced with the same challenges, embryonic teleosts such as rainbow trout (*Oncorhynchus mykiss*) do not completely develop these systems until after hatching. Yet, there is evidence that ion regulation occurs in embryonic and larval salmonids. For example, Shen and Leatherland (1978) measured significant accumulations of Na^+ and K^+ in rainbow trout embryos. Similarly, Misiaszek (1996) found significant accumulations of Na^+, Ca^{2+}, and Cl^- in larval rainbow trout. Also, a few studies have shown that embryos and larvae are capable of maintaining ionic homeostasis under conditions which normally disrupt ion balance. In particular, salmonid embryos and larvae maintained constant levels of ions during exposure to deionized water, 13% sea water (Shen and Leatherland, 1978)

and low levels of toxic trace metals such as aluminum and cadmium (Rombough and Garside, 1984; Wood *et al.*, 1990). Of all the early life stage studies, very few have been concerned with the development of ionoregulatory mechanisms prior to hatching.

Morphology of Salmonid Eggs

Typical salmonid eggs consist of a developing embryo and its associated yolk sac (Figure 1.1). In freshly fertilized eggs, the yolk sac contains 76.9% of whole egg protein, 92.2% of whole egg lipid, and 2% of whole egg carbohydrate (Heming and Buddington, 1988). Protein catabolism from the yolk sac is the primary source of energy for endogenously feeding embryos and larvae (Kamler, 1992; Heming and Buddington, 1988; Wright *et al.*, 1995; Rahaman-Norohna *et al.*, 1996).

Surrounding the embryo and yolk sac is a tough, but elastic acellular outer shell called the chorion or zona radiata. It has been argued that the chorion is permeable to small inorganic ions such as H^+, Na^+, Ca^{2+}, K^+, and Cl^-, and compounds such as water, and NH_3, but is relatively impermeable to substances of higher molecular weight (Eddy, 1974; Peterson and Martin-Robichaud, 1987, 1992; Rahaman-Norohna *et al.*, 1996).

Between the chorion and embryo is a perivitelline space which is formed minutes after exposure of an unfertilized egg to water (Eddy, 1974). It is believed that as eggs are shed into freshwater, the ionic and osmotic shock triggers the separation of the vitelline membrane from the chorion. Concurrently, macromolecules and ions are released from the yolk into the perivitelline space, forming the colloidal perivitelline fluid (pvf) (Eddy,

Figure 1.1: A typical salmonid egg.

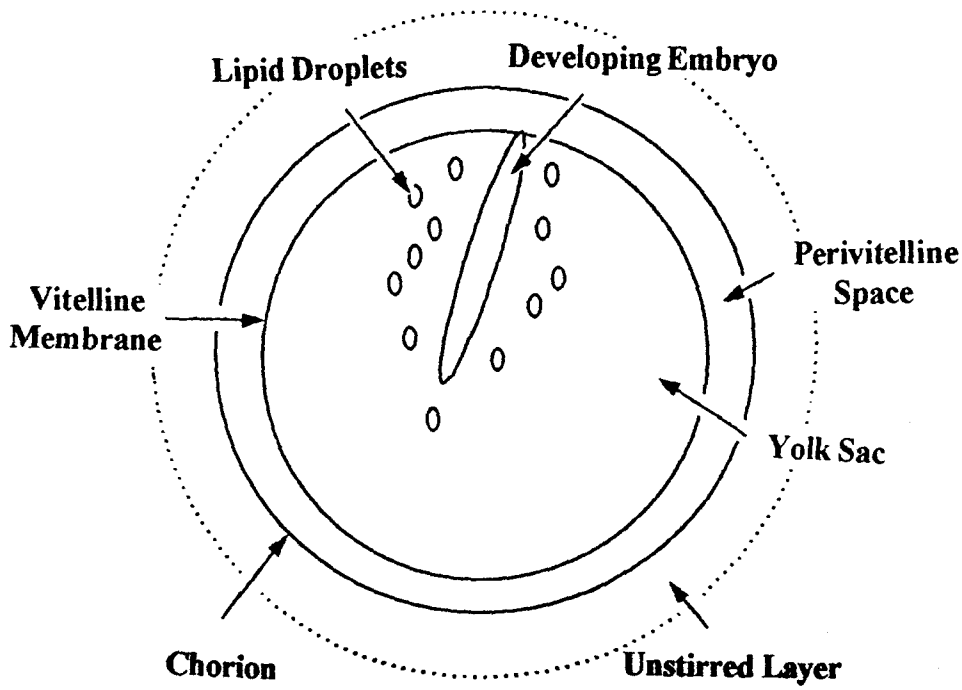
Lipid Droplets
Developing Embryo
Perivitelline Space
Vitelline Membrane
Yolk Sac
Chorion
Unstirred Layer

1974; Alderdice, 1988). The composition of the pvf in Atlantic salmon eggs is 58% water, 25% protein, 12% lipid, and 1.7% carbohydrates (Eddy, 1974; Alderdice, 1988).

The pvf and chorion function to protect the developing embryo from mechanical shock and abrasion (Alderdice, 1988)

Contribution of Chorion and PVF to Ion Regulation

The embryo is exposed directly to conditions in the pvf, rather than the surrounding water. It has been suggested that the chorion has ion exchange properties and that the permeability is higher for H^+, K^+, and Cl^-, than for Na^+ and Ca^{2+} (Peterson and Martin-Robichaud, 1987). This would create a pvf 'environment' which has a different ionic composition than that of the surrounding water. In addition, Kugel and Peterson (1989) found that the pvf showed a significant buffer capacity when exposed to water of various pH. They suggested that the perivitelline colloids act as the primary buffer substance. The ability to act as a buffer, especially at low external pH, allows the pvf to protect the developing embryo from drastic changes in water pH.

At normal external and internal pH, the pvf is predominantly acidic and negatively charged and there is a tendency for it to accumulate cations in excess of the external concentration (Eddy and Talbot, 1985; Alderdice, 1988; Kugel and Peterson, 1989; Shephard, 1987). These anionic charges are likely produced by the weak acid groups on the pvf macromolecules (Shephard, 1987).

Eddy and Talbot (1985) removed the chorions from salmon eggs and found a dramatic increase in loss of Na^+ from the embryo. In addition, Shen and Leatherland (1978) found that rainbow trout eggs reared in 13% sea water developed normally, but when they began to hatch, many of the embryos died.

More recently, however, Ayson *et al.* (1994) investigated the role of the chorion and pvf in ion and osmoregulation in embryonic teleosts. They found that if tilapia (*Oreochromis mossambicus*) eggs reared in freshwater are dechorionated and placed in sea water, the embryos survive. This suggests that, in spite of the possible contribution of the pvf and chorion to ion transfer across the egg, the regulatory capacity is not completely dependent on egg shell permeability or pvf composition. Rather, the embryo itself must possess some mechanism for maintaining ionic homeostasis.

Contribution of Embryo to Ion Regulation

Prior to the development of a complete renal complex, gut and branchial epithelium, the cutaneous surfaces (i.e. body and yolk sac) of developing embryos are the probable sites of ion regulation. There have been very few studies on the development of ion regulation at the surface of salmonid embryos. Most evidence points to the presence of specialized mitochondria-rich cells (MRCs), also known as chloride cells, which actively transport ions across epithelial surfaces. These cells are responsible for much of the ion regulation in adult teleosts (Karnaky, 1986; Avella *et al*, 1987; Perry, 1992; Zadunaiski, 1988).

Freshwater chloride cells characteristically have a shallow apical crypt which faces the surrounding water, and an extensive tubular vesicular system which develops from the basolateral membrane (Alderdice, 1988; Zadunaiski, 1984). These cells also contain numerous mitochondria which provide the energy necessary to actively transport ions against the concentration gradient between the body fluids and external water (Alderdice, 1988). Tight junctions at the epithelial surface join adjacent chloride cells.

Although the basic morphology of chloride cells has been described, relatively little is known about the development of these cells or their role in embryonic teleosts. MRCs have been found in embryos and larvae of ayu, carp, flounder (Hwang and Hirano, 1985; Hwang, 1989), tilapia (Li *et al.*, 1995; Ayson *et al.*, 1994; Hwang *et al.*, 1994), and rainbow trout (Shen and Leatherland, 1978; Misiaszek, 1996). These cells may be located in the pectoral fin, yolk sac, pericardial, tail, or branchial regions of embryos and larvae (Shen and Leatherland, 1978; Hwang, 1989; Ayson *et al.*, 1994; Li *et al.*, 1995; Misiaszek, 1996).

A few studies have shown that changes in MRC morphology occur when embryos and larvae are placed in water of various salinities. Hwang and Hirano (1985) and Ayson (1994), for example, determined that when larval ayu and tilapia were reared in freshwater and transferred to sea water, MRCs developed characteristics of sea water MRCs. Although this phenomenon has been investigated in only a few species, it is likely that chloride cells contribute to the ionoregulatory ability of embryonic and larval fish.

Respiration and Metabolism in Embryonic Salmonids

Relatively little is known about respiratory gas exchange and metabolism during early life stages in teleosts. In rainbow trout, there appears to be a 50% increase in oxygen consumption after fertilization, and a further 4-fold increase by the end of epiboly (Boulekebache, 1981). Rombough (1988) suggests that fertilization, gastrulation, formation of embryonic circulation, and hatching are the events during embryonic development most likely to alter the rate of metabolic oxygen consumption. There is controversy, however, about the extent of changes in metabolic rate prior to hatching. Some studies report increases in metabolic rate over the last stages of development, while others report decreases or no change in metabolic rate (Rombough, 1988).

Regardless, the passing of respiratory gases (i.e. O_2 and CO_2) and metabolic products (i.e. NH_3/NH_4^+) across epithelia can be described using a cascade model (Rombough, 1988). This model suggests that materials pass through a series of resistances, each of which is associated with a specific process or structure (i.e. pvf, chorion, boundary layer). The overall resistance of the system is the sum of the individual resistances and under steady-state conditions, the overall flow through the system is the flow through any one of the structures (Rombough, 1988). Although there is little information about respiration in embryonic teleosts, this model can be used to identify and describe the major resistances during development.

Contribution of Chorion and PVF to Respiratory and Metabolic Gas Exchange

The chorion was originally thought to be the major barrier to diffusive gas exchange during embryonic development. With the recent use of microelectrode techniques, it has been shown clearly that the pvf has a much greater resistance to gas exchange than does the chorion (Rombough, 1988). Therefore, the rate of oxygen consumption, carbon dioxide excretion and metabolic waste excretion are affected considerably by the properties of pvf and chorion, since these layers act as barriers for exchange of materials between embryos and the environment.

Contribution of Gills and Cutaneous Surfaces to Gas Exchange

The gills are a major site of respiratory gas and metabolic product transfer in adult teleosts (Rombough, 1988). Prior to hatching, however, gills may not be fully developed. Gill development appears to differ with different freshwater species. For example, it has been shown that gill arches and filaments are completely developed by hatching in rainbow trout (*Salmo gairdneri*) (Morgan, 1974). In newly hatched Arctic char, however, filaments are unevenly distributed among the four gill arches and secondary lamellae are not developed (McDonald and McMahon, 1977). Recently, Wells and Pinder (1996) determined that gills are poorly developed in newly hatched Atlantic salmon. Only a few of the fish sampled (2 out of 6) had lamellae that could be measured.

Whether or not gills are fully developed prior to hatching, it is clear that the cutaneous surface, not the branchial surface, is largely responsible for the majority of

respiratory gas exchange (Wells and Pinder, 1996; Rombough, 1988; Rombough, 1998; Rombough and Ure, 1991). The morphological potential for gas exchange across skin and gills is determined by surface area and blood-water barrier thickness according to Fick's law of diffusion:

$$\textbf{Gas Exchange} = (A/D)*K*\Delta P_{gas}$$

where **A** is the surface area, **D** is the thickness of the water-blood barrier, **K** is Krogh's diffusion coefficient and ΔP_{gas} is the difference in partial pressures of the gas between the blood and respired water (Wells and Pinder, 1996).

Rombough and Ure (1991) and Wells and Pinder (1996) determined that shortly after hatch, approximately 80% of all oxygen consumed by larval Chinook and Atlantic salmon was taken up across the skin. The skin can be partitioned into the yolk sac and body surface. It is expected that due to its vascularization, large surface area, and thin epithelium compared to the body surface, the yolk sac would be the predominant gas exchange surface in embryonic and larval salmonids. Wells and Pinder (1996) showed, however, that of the total oxygen uptake across larval surfaces, the yolk sac was responsible for only 33%, whereas the developing tissue (body) was responsible for the remainder. Similar studies for CO_2 excretion have not been done.

Unstirred Layers

There is evidence that unstirred layers (USLs), or boundary layers, may have an effect on respiratory gas exchange in aquatic organisms (Rombough, 1998; Pinder and

Feder, 1996; Rombough, 1988). USLs are semistagnant regions of water adjacent to an organism where oxygen is depleted and metabolic wastes are accumulated (Rombough, 1988). They expose an organism directly to a microenvironment which does not have the same composition as the external medium (i.e. lower P_{O2}, higher P_{CO2} and concentration of metabolic wastes such as NH_3/NH_4^+) (Randall and Wright, 1989).

In adult rainbow trout, it has been determined that the USL adjacent to the gills is acid relative to the bulk water (Wilson *et al.*, 1994). This acidification is attributed to the hydration of excreted CO_2 and/or direct H^+ transport. As CO_2 is excreted across the gills, it becomes hydrated to form HCO_3^- and H^+, the latter of which acidifies the water adjacent to the gills (Wilson *et al.*, 1994; Randall and Wright, 1989). The hydration reaction is catalysed by carbonic anhydrase found in the mucous layer around the gills (Misiaszek, 1996). There is some evidence for the presence of an acid USL adjacent to rainbow trout eggs (Rahaman-Norohna *et al.*, 1996) and larvae (Misiaszek, 1996), but the exact mechanism of its formation is unclear.

CO_2 (from respiration) and NH_3 (from catabolism of yolk sac proteins) are the major metabolic end products in adult and embryonic teleosts (Randall and Wright, 1989, Rahaman-Norohna *et al.*, 1996; Wright, 1995; Wright *et al*, 1995). There is very little information in the literature on sites or extent of CO_2 excretion or on the transport and distribution of NH_3/NH_4^+ within fish eggs. It is clear, however, that ammonia movement across most biological membranes is primarily by NH_3 diffusion down the partial pressure gradient (Rahaman-Norohna *et al.*, 1996; Wright, 1995; Randall and Wright, 1989). If

NH_3 is excreted into an acid compartment (such as the acid USL adjacent to the gills of adult fish, or chorions of eggs), it becomes protonated to form NH_4^+. This promotes further excretion of NH_3. The relationship between NH_3 excretion, $[NH_4^+]$ and pH of the USL adjacent to embryos has not been investigated.

Organization and Objectives

It is the purpose of this study to investigate the development of ion regulation and USL acidification in embryonic rainbow trout (*Oncorhynchus mykiss*). In addition, the possible roles of the chorion and pvf in these processes will be addressed. Chapter 2 will investigate the amount and distribution of water and electrolytes in whole eggs from fertilization to hatch. In addition, it will describe patterns of Na^+, Ca^{2+}, and Cl^- accumulation in whole eggs, and characteristics of Na^+ and Ca^{2+} uptake in whole eggs and dechorionated embryos. Chapter 3 will investigate properties of USL adjacent to eggs and dechorionated embryos; the measurement of parameters such as pH, $[NH_4^+]$ and P_{CO2} in the USL at various locations around eggs and dechorionated embryos will provide insight into the sites of production and extent of excretion of these materials. Finally, chapter 4 will summarize the major arguments from chapters 2 and 3, suggest applications of techniques demonstrated in this study, and recommend areas of future research.

CHAPTER 2: ION CONTENT AND TRANSPORT IN EMBRYONIC RAINBOW TROUT

INTRODUCTION

There is relatively little information in the literature on the development of ion regulation in early life stages of freshwater fish, especially in the period before hatching. Basic information, such as characteristics of water and electrolyte content and distribution within eggs, is lacking.

The ability of eggs and embyros to accumulate, redistribute, and lose Na^+, has been demonstrated by only a few studies (i.e. Rudy and Potts, 1969; Shen and Leatherland, 1977; Eddy and Talbot, 1985; Shephard and McWilliams, 1993; McWilliams, 1993). Most of these papers investigated the nature of Na^+ uptake at a single developmental stage, and not the patterns of whole egg uptake, distribution, and accumulation throughout development.

Studies of Ca^{2+} balance in embryonic teleosts have included very few species and have been concerned primarily with morphological changes of chloride cells (MRC), or with changes in pvf [Ca^{2+}] associated with changes in external calcium concentration (Hwang *et al.*, 1994; Shephard, 1987). The basic properties of Ca^+ balance in embryos have not been investigated for rainbow trout; there is a lack of evidence for whole egg Ca^{2+} content, distribution, uptake and loss. Similarly, properties of whole egg Cl^- content and distribution have not been determined.

It is the purpose of this chapter to determine some of the basic properties of whole egg ion and water content during embryonic development of rainbow trout (*Oncorhynchus mykiss*). In particular, patterns of accumulation and distribution of Na^+, Ca^{2+}, and Cl^- are investigated using whole eggs and dechorionated embryos at various stages of embryonic development. In addition, radiotracer studies are used to determine the extent and possible mechanism of Na^+ and Ca^{2+} exchange across surfaces of whole eggs and dechorionated embryos. The potential roles of pvf and chorion will also be discussed.

MATERIALS AND METHODS

Experimental Animals

Rainbow trout eggs were obtained either freshly fertilized or 'eyed-up' (Table 2.1) from Rainbow Springs Trout Farm in Thamesford, Ontario. All egg lots were held in 500 mL square containers with a constant flow of aerated, dechlorinated Hamilton tap water ($[Na^+]$= 0.6 mmol l^{-1}; $[Cl^-]$= 0.7 mmol l^{-1}; $[HCO_3^-]$= 1.9 mmol l^{-1}; pH 7.9), chilled to 7°C ± 1°C throughout all experimental periods. The containers were covered to maintain low light levels and dead eggs, indicated by their whitish opaque colour, were removed daily.

Dechorionating Embryos

Some of the experiments required removal of the chorion, or egg shell, from *O. mykiss* embryos in order to provide direct access to the developing embryos. Dechorionating by dissection was not possible until the eye pigmentation stage had begun. Using a dissecting microscope (16x magnification), a 0.25mm slit was made in the chorion with a sharp 18- or 25- gauge syringe needle. The incision was made in the chorion close to the head of the embryo where the perivitelline space was most evident. It was much more difficult to dechorionate younger eggs (early eye pigmentation stage) than older eggs because the yolk sac was more delicate and the perivitelline space was less accessible. As a result, it was necessary to make very small and shallow incisions at this stage.

Table 2.1: Key developmental stages in embryonic rainbow trout maintained at $7 \pm 1°C$ in Hamilton tap water ($[Na^+]$= 0.6mmol l^{-1}; $[Cl^-]$= 0.7mmol l^{-1}; $[HCO_3]$= 1.9mmol l^{-1}; pH 7.9).

Days Post Fertilization	Event
0	Fertilization
14	Embryo seen through chorion without aid of microscope
21-28	Eye pigmentation
45-55	Hatching

Once the small incision was made, one pair of sharp forceps was used to grip a cut edge of chorion, while another pair was used to make small tears in the egg shell. The yolk sac was easily ruptured if the cut edge of the chorion either contacted or compressed the yolk sac. As a result, only small strips of chorion were removed at a time until the embryos could free themselves from the remaining egg shell. In older eggs (fully eyed, near hatch), ruptures in the yolk sac occured less frequently. At this stage, dechorionations were accomplished with greater ease by tearing relatively large strips of chorion from the egg.

Whole Egg Water Content

Every 3-4 days, from the day after fertilization to the day of hatch, 5 eggs were sampled at random from holding containers for determination of whole egg wet weight, dry weight and water content. To determine wet weight, each egg was blotted dry on paper towel to remove surface moisture and weighed on a tared balance in a 1.5ml centrifuge tube. Weighed eggs were stored in a freezer for subsequent dry weight measurements.

Dry weight was determined after the frozen eggs were placed in a 60°C oven for 48 hours and cooled in a dessicator. Eggs were weighed individually and whole body water content was calculated using the following equation:

Water Content= 100* ((Wet Weight- Dry Weight)/Wet Weight)

where water content was expressed as % wet weight and all weights were expressed as mg.

Whole Egg Ion Content

At 3-4 day intervals, 5 eggs were sampled at random for whole body Na^+, Ca^{2+}, and Cl^-. Each egg was blotted dry, weighed, placed in a 1.5 ml centrifuge tube, and digested in 500µl 1N H_2SO_4. Samples were stored for later analysis.

Distribution of Na^+, Ca^{2+}, and Cl^- Within Whole Eggs

The distributions of Na^+, Ca^{2+}, and Cl^- within developing eggs were determined using a single egg lot. Every 4 days from 28 days after fertilization to hatching, 15-20 eggs were selected at random and divided between 3 treatments. In the first treatment, 5 eggs were blotted dry, weighed, and digested in 500µl 1N H_2SO_4. In the second treatment, 5 eggs were blotted dry, weighed, and dechorionated in H_2O_{dd} . The whole embryo was then blotted dry, weighed and digested in 500µl 1N H_2SO_4. In the third treatment, 5 eggs were blotted dry, weighed and dechorionated as above. The whole embryos and yolk sacs were weighed individually and the yolk sacs were carefully removed from the embryo using two pairs of fine forceps. The yolk sacs were discarded and the remaining tissue was blotted dry, weighed and digested in 500µl 1N H_2SO_4.

Samples were discarded if there was excessive blood loss and/or yolk leakage. The fluid was precipitated with ethanol and removed with forceps. Digested samples were stored for subsequent ion analysis.

Analytical Methods

Digested samples were mixed in centrifuge tubes with a clean spatula, vortexed and centrifuged (1500 x g, Fisher Scientific) for 5 minutes. Prior to measurement of Na^+ concentration, 60µl of the supernatant from each centrifuged sample was diluted in 1.5 ml H_2O_{dd}. For Ca^{2+}, 50µl of the supernatant was diluted in 5 ml H_2O_{dd} and 100 µl 10% $LaCl_3$. Cl^- analysis did not require sample dilution. Na^+ and Ca^{2+} concentrations were determined using a Varian AA-1275 Series atomic absorbance spectrophotometer and Cl^- samples were analyzed using a model CM 10 chloride titrator (Radiometer-Copenhagen).

Na^+ Uptake Kinetics

Na^+ uptake kinetics were measured in whole eggs and dechorionated embryos to determine whether a Na^+ transport mechanism exists in rainbow trout prior to hatch. At various stages of late embryonic development, 5 whole eggs and 5 dechorionated embryos were exposed for 3 hours to one of 6 concentrations of Na^+ (ranging from 0.05 to 2.5 mmol l^{-1} NaCl in 1.0 mmol l^{-1} $CaCl_2$, pH adjusted to 7.9 with KOH). Embryos were dechorionated 30-60 minutes prior to each experiment, and were maintained at 7^0C in subdued light until they were placed in the aerated experimental media. Eggs and

dechorionated embryos were rinsed in deionized water before each experiment to remove surface bound ions. $^{24}Na^{+}$ was added to each solution in concentrations ranging from 0.09 μCi/ml to 4.5 μCi/ml.

Water samples were taken at the start and end of the experiment, to determine specific activity and Na^{+} concentration of the radiolabelled media.

At the end of the exposure period, animals were rinsed in deionized water to remove surface bound $^{24}Na^{+}$, weighed on a tared balance and placed in individual scintillation vials. The samples were counted in a Minaxi auto gamma 5000 series gamma counter (Canberra- Packard Canada, Ltd.).

Ca^{2+} Uptake Kinetics

As for Na^{+}, Ca^{2+} uptake kinetics were measured in whole eggs and dechorionated embryos to determine the extent of Ca^{2+} accumulation in rainbow trout prior to hatch. Groups of 5 eggs and 5 dechorionated embryos were exposed to one of 6 bathing solutions containing 0.65 mmol l^{-1} NaCl and concentrations of Ca^{2+} ranging from 0.005 mmol l^{-1} to 1.25 mmol l^{-1} $CaCl_2$ (pH adjusted to 7.0 with NaOH). Each solution was radiolabelled with $^{45}Ca^{2+}$ concentrations ranging from 0.0017 μCi/ml to 0.43 μCi/ml.

Water samples were taken at the start and end of the exposure period to determine specific activity and $[Ca^{2+}]$ of the experimental solutions. Animals were rinsed in deionized water prior to being placed in the experimental media. At the end of the 3 hour exposure, each animal was rinsed briefly in a 10 mM EDTA solution to remove surface

bound $^{45}Ca^{2+}$, weighed on a tared balance, and placed in individual scintillation vials with 1ml of tissue solublizer (Soluene- 350, Packard- Canberra Canada, Ltd.). The vials were placed in a 60^0C oven overnight to accelerate tissue digestion.

$^{45}Ca^{2+}$ activity was determined by adding 10 ml of a liquid scintillation fluor (Hionic-Fluor, Packard- Canberra Canada, Ltd.) to both water and animal samples. The vials were shaken and placed in a beta-counter (1217 RackBeta liquid scintillation counter, LKB Wallac, Fisher Scientific).

Na^+ Efflux

At 32 days post fertilization, eggs were selected at random for determination of Na^+ efflux. Twenty eggs and 20 dechorionated embryos were placed in aerated solutions of 2.5 mmol l^{-1} NaCl in 1.0 mmol l^{-1} $CaCl_2$ (pH 7.9) with 4.5μCi/ml $^{24}Na^+$ for 3 hours. Eggs were dechorionated 30 minutes prior to the experiment and any showing damage were discarded. Water samples were taken at the start and end of the experiment to determine specific activity and Na^+ concentration of the medium. After 3 hours, each egg and embryo was rinsed briefly in deionized water to remove surface bound Na^+, then placed in a volume of non-radiolabelled Hamilton tap water. At several time intervals (30 min, 1 h, 2h, 4h), 5 eggs and 5 embryos were removed and counted as above (Na^+ uptake kinetics).

Ca^{2+} Efflux

Methods were similar to those for the Na^+ efflux experiment, but the eggs and embryos were loaded in a solution of 1.25 mmol l^{-1} $CaCl_2$ in 0.65 mmol l^{-1} NaCl (pH 7.4) with 0.43 μCi/ml $^{45}Ca^{2+}$ for 3 hours. After the 3 hour exposure, each egg and embryo was rinsed briefly in 10 mmol l^{-1} EDTA and placed in non-radiolabelled Hamilton tap water. Animals were sampled at the same intervals as described above, and were rinsed again in 10 mmol l^{-1} EDTA prior to being weighed and placed in individual scintillation vials with 1 mL tissue solublizer (Soluene- 350, Packard- Canberra Canada, Ltd.). Tissue and water samples were digested and counted as described for Ca^{2+} uptake kinetics.

Data Analysis for Na^+ and Ca^{2+} Kinetics

Na^+ and Ca^{2+} influx and efflux rates ($J_{in/out}^{Na+}$ and $J_{in/out}^{Ca+}$) were determined based on the accumulation or loss of radioactivity in the whole egg and dechorionated embryo using the equation:

$$J_{in} = (CPM)/(SA*W*t)$$

where **CPM** was the counts per minute per egg or dechorionated embryo, **SA** was the specific activity of the water (cpm/nEq), **W** was the wet weight of the egg or dechorionated embryo (g), and **t** was the duration of exposure to radiolabelled media (hours).

Kinetic parameters, J_{max} and K_m were determined in SAS JMP using the following equation:

$$J_{in} = J_{max} * [ion] / (K_m + [ion])$$

where J_{in} was the Na^+ or Ca^{2+} uptake rate and **[ion]** was the external concentration of Na^+ or Ca^{2+}.

Statistical Analysis

Differences between two means were compared using student t-tests. Differences between more than two means were analysed using either 1-way or 2-way analysis of variance (ANOVA). Tukey and least standard difference (LSD) post-hoc tests were then performed to determine significance between variables. Differences were judged to be significant if $p<0.05$.

RESULTS

Whole Egg Water Content and Distribution of Wet Weight

Although there were significant differences in wet and dry weights of eggs between lots (t-test, $p < 0.05$), water content remained the same (Table 2.2). Amongst the first 4 lots sampled, the average wet and dry weight was 55.6 and 19.7 mg, respectively. Mean dry weight was 35.6% wet weight, and mean water content was 64.4%.

There was not a significant variation in water content within each egg lot as a function of age (ANOVA, $p>0.05$). There were, however, changes in the distribution of wet mass within each egg during embryonic development (Figure 2.1). Tissue mass (embryo minus yolk sac) increased significantly from 9.43% to 13.02% of the total embryo wet mass between day 40 and day 52 (ANOVA, $p < 0.05$). However, whole embryo, pvf and chorion contribution to whole egg weight did not change over the same period (ANOVA, $p<0.05$). At 40 days after fertilization, the whole embryo contained 86.7% of the whole egg wet mass, while the perivitelline fluid and chorion together contained 13.3%. There were no significant changes in these values or in the yolk sac mass between day 40 and 52 (ANOVA, $p > 0.05$).

Table 2.2: Summary of whole egg wet weight, dry weight, and % water content during embryonic development in different egg lots. Means ± SE, n-values reported in table.

Group	Wet Weight (mg) ±SE	Dry Weight (mg) ±SE	% Water Content ±SE	n
1	49.59 ± 0.93	17.29 ± 0.26	64.83 ± 0.5	53
2	70.42 ± 1.23	25.44 ± 0.59	63.89 ± 0.51	19
3	60.64 ± 2.63	22.07 ± 1.07	63.73 ± 0.49	24
4	49.47 ± 1.17	16.93 ± 0.37	65.66 ± 0.61	14
5	93.47 ± 0.60	-	-	20

Figure 2.1: Distribution of wet weight in eggs over the last 12 days of embryonic development. Eggs from group 5 in table 2.2. Means ± SE, n=5.

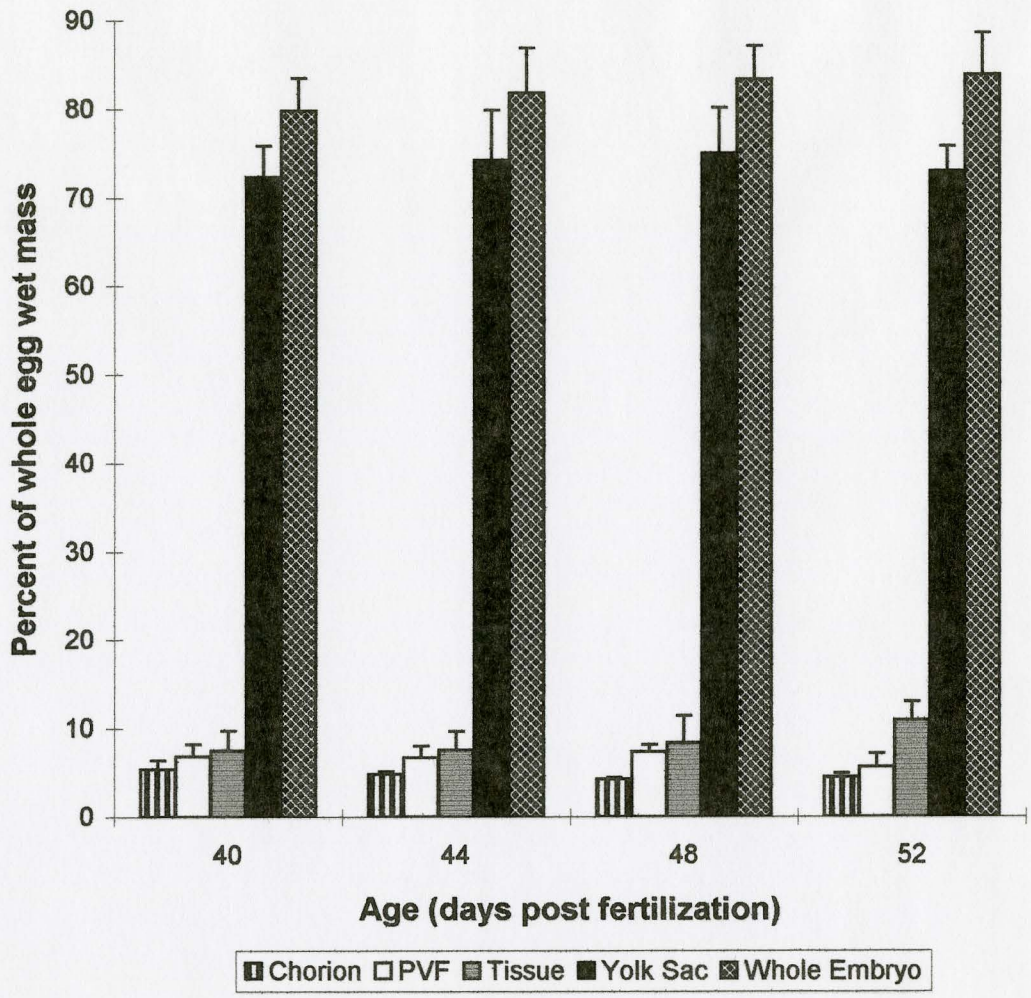
Percent of whole egg wet mass
90
80
70
60
50
40
30
20
10
0
40
44
48
52
Age (days post fertilization)
Chorion
PVF
Tissue
Yolk Sac
Whole Embryo

Whole Egg Ion Content

Electrolyte content increased linearly with dry weight (Figure 2.2). Total Ca^{2+} ranged from 1.43 ± 0.040 to 1.60 ± 0.14 μEq/egg; Cl^- from 0.88 ± 0.041 to 1.37 μEq/egg; Na^+ from 0.86 ± 0.050 to 1.07 ± 0.070 μEq/egg. Whole egg electrolyte content was measured on 4 separate egg lots and results from all lots were pooled to determine overall trends. In general, whole eggs contained more Ca^{2+} and Cl^- than Na^+. However, for the last 10 days of development, eggs had equal amounts of Na^+ and Cl^- (Figure 2.3) (ANOVA, $p>0.05$).

Although Na^+, Ca^{2+}, and Cl^- contents remained constant at the beginning of embryonic development, eggs in some lots accumulated these electrolytes near the end of embryonic development (i.e. between 0 and 20 days before hatch). The net accumulation over the last 20 days of embryonic development was best described by the following exponential relationship:

$$[ion] = ae^{bt}$$

where **[ion]** was whole egg ion content (μEq/egg), **t** was the age (days), **b** was an accumulation rate (% day^{-1}) and **a** was a constant.

All 4 lots showed accumulation of Na^+ (Table 2.3). Changes in Ca^{2+} and Cl^- were variable; different lots gained, lost, or showed no change in the levels of these ions.

Figure 2.2: Relationship between whole body Na^+, Ca^{2+}, and Cl^- content (uEq/egg) and dry weight (mg) during embryonic development. Y-Intercept is near zero (-1.18 to 0.57) for each plot. Means ± SE; n= 6.

A. Na^+ relationship described by equation $y = 0.0688x - 0.3681$, $R^2 = 0.332$.

B. Ca^{2+} relationship described by equation $y = 0.047x + 0.5734$, $R^2 = 0.437$.

C. Cl^- relationship described by equation $y = 0.124 - 1.182$, $R^2 = 0.778$

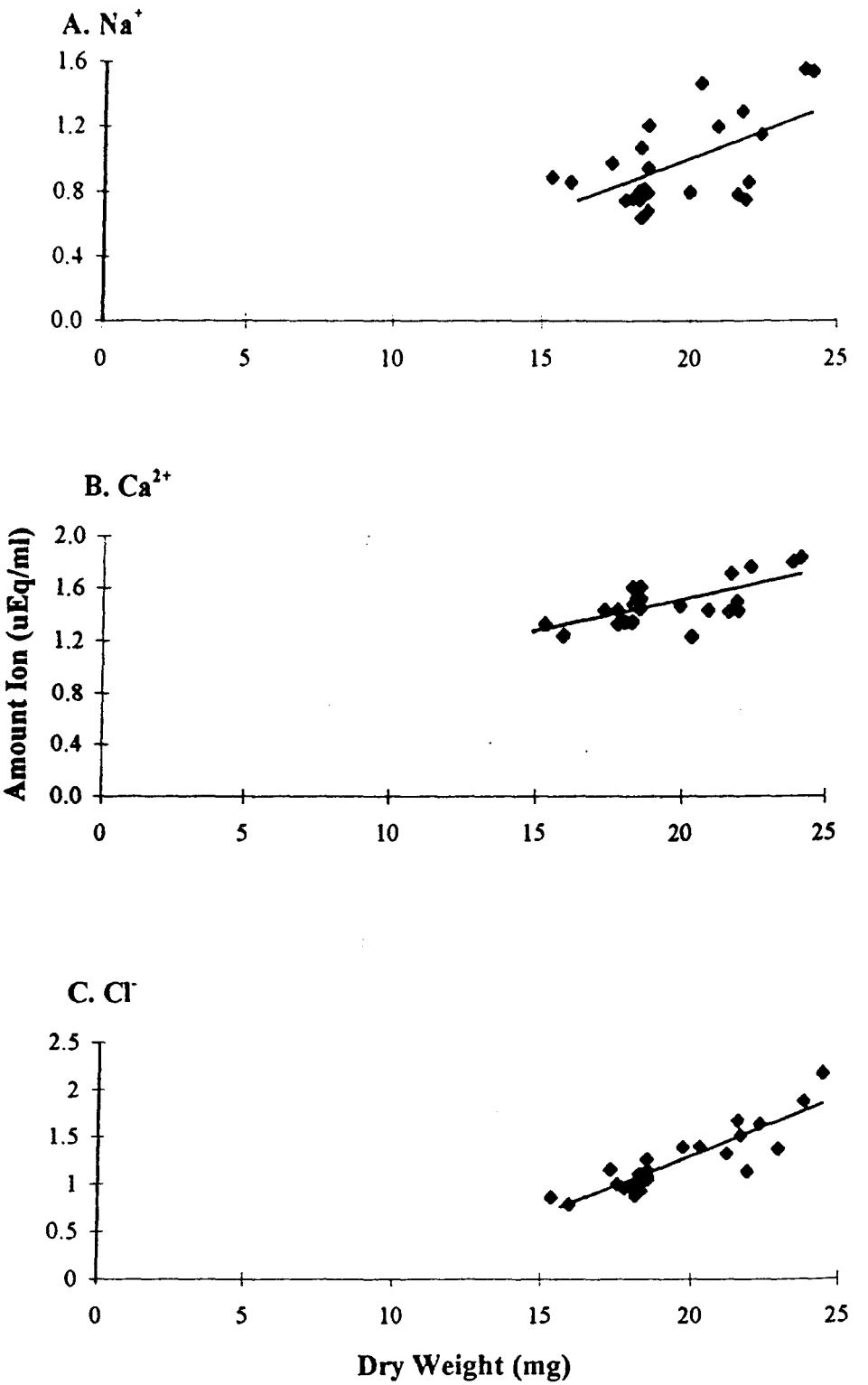
A. Na+
1.6
1.2
0.8
0.4
0.0
0
5
10
15
20
25
B. Ca2+
Amount Ion (uEq/ml)
2.0
1.6
1.2
0.8
0.4
0.0
0
5
10
15
20
25
C. Cl-
2.5
2
1.5
1
0.5
0
0
5
10
15
20
25
Dry Weight (mg)

Figure 2.3: Relationship between whole egg Na^{+}, Ca^{2+}, and Cl^{-} content ($\mu Eq*egg^{-1}$) and age from fertilization to hatch in 4 egg lots. Means ± SE, n=20 for day 0-20 before hatch; n=5 for day 21-50 before hatch.

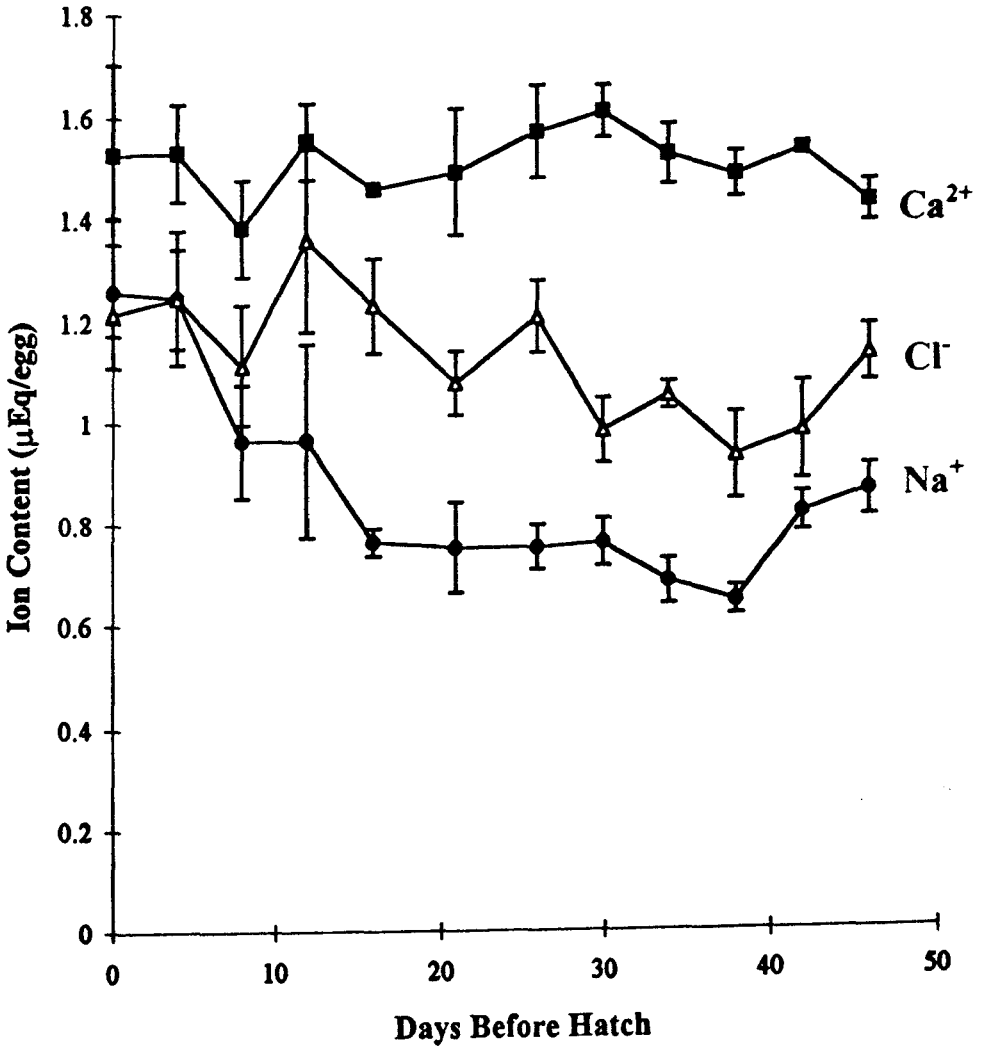
1.8
1.6
1.4
1.2
1
0.8
0.6
0.4
0.2
0
Ion Content (μEq/egg)
0
10
20
30
40
50
Days Before Hatch
Ca2+
Cl-
Na+

Table 2.3: Whole egg Na^+, Ca^{2+}, and Cl^- accumulation rate (% day^{-1}) over the last 20 days of embryonic development in 4 egg lots. R^2 determined for fit to the function $[ion]=ae^{bt}$. Lot 1 was raised from fertilization to hatch. Lots 2, 3, and 4 were raised from day 12-16 after fertilization to hatch.

Egg Lot	Na^+ Accumulation Rate (%day^{-1}) ± SE		Ca^{2+} Accumulation Rate (%day^{-1}) ± SE		Cl^- Accumulation Rate (%day^{-1}) ± SE	
	Rate	R^2	Rate	R^2	Rate	R^2
1	1.9 ± 0.2	0.70	0.4 ± 0.1	0.12	-0.8 ± 0.2	0.18
2	2.6 ± 0.1	0.88	0.4 ± 0.1	0.54	2.7 ± 0.2	0.75
3	4.2 ± 0.3	0.96	-0.8 ± 0.1	0.55	-0.2 ± 0.1	0.002
4	2.0 ± 0.1	0.61	1.5 ± 0.1	0.99	1.6 ± 0.1	0.95

Distribution of Na^+, Ca^{2+}, and Cl^- in Whole Egg

A single egg lot was used to determine electrolyte distribution within whole eggs. At 32 days post fertilization, 72% of whole egg Na^+ was concentrated in the embryo, whereas only 28 % was in the chorion and perivitelline fluid. The amount of Na^+ in the embryo increased significantly to 92% of whole egg Na^+ by 52 days post fertilization, leaving only 8% in the chorion and perivitelline fluid (Figure 2.4) (t-test, $p<0.05$). For the last 12 days of embryonic development, 59.1 ± 9.4% of the whole egg Na^+ was located within the yolk sac. Although yolk sac Na^+ content did not change, the tissue Na^+ content (embryo minus yolk sac) increased 46.8% over this period (t-test, $p<0.05$).

The distribution of Cl^- within the egg also changed between day 40 and 52 (Figure 2.5). Although there were no changes in whole embryo Cl^-, the distribution of Cl^- between the yolk sac and tissue changed; between day 40 and 52; the contribution of yolk sac to whole egg Cl^- decreased significantly from 54.2 ± 3.4% to 38.8 ± 2.1% (t-test, $p<0.05$), while contribution of tissue increased significantly from 43.2 ± 2.2 to 54.1 ± 2.4% (t-test, $p<0.05$).

The distribution of Ca^{2+} did not change significantly over the last 12 days of embryonic development (Figure 2.6). The embryo contained 96.86 ± 1.9% of whole egg Ca^{2+} at day 40 and 93.36 ± 3.68% at day 52. Approximately 35% of the whole embryo Ca^{2+} was found in the tissue, while 65% was in the yolk sac. This distribution did not change between day 40 and day 52. Together, the pvf and chorion contained 3.14% and 6.64% of whole egg Ca^{2+} at day 40 and 52, respectively.

Figure 2.4: Distribution of Na^+ between whole egg, embryo, yolk sac, and tissue over the last 12 days of embryonic development. Means ± SD, n=5.

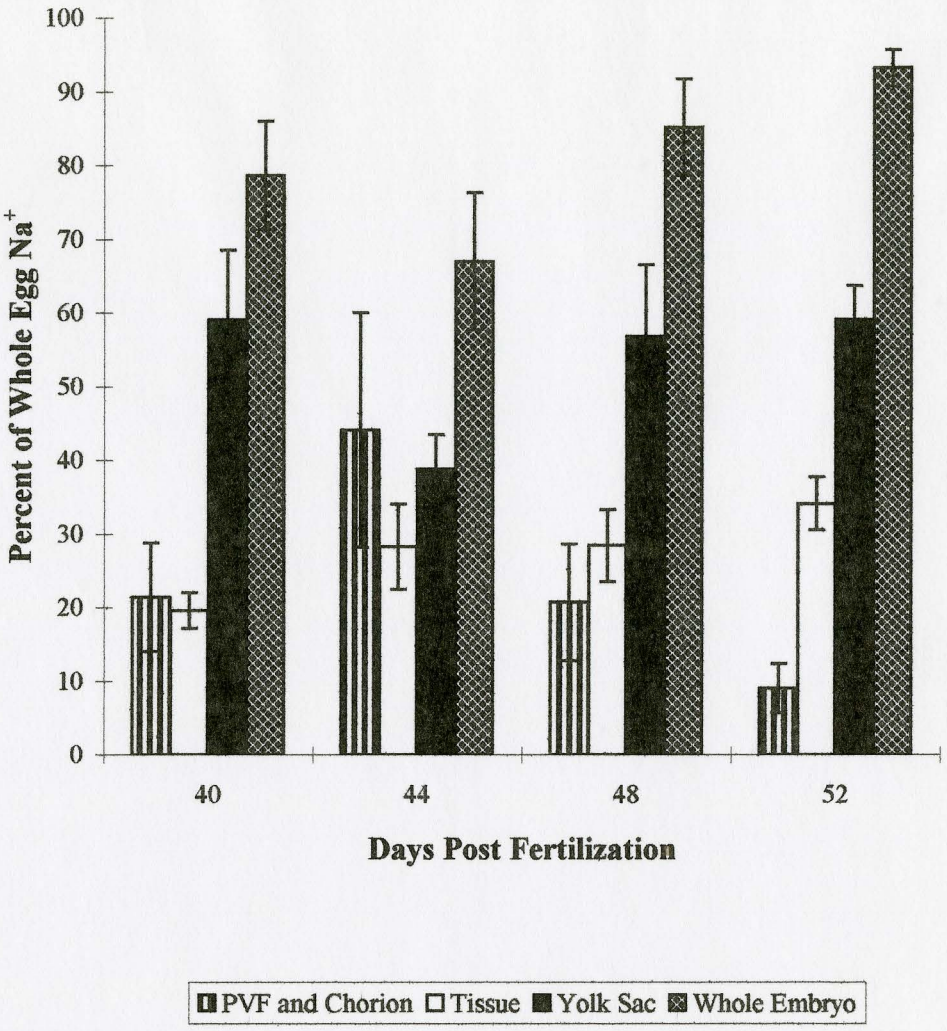
100
90
80
70
60
50
40
30
20
10
0
Percent of Whole Egg Na+
40
44
48
52
Days Post Fertilization
PVF and Chorion
Tissue
Yolk Sac
Whole Embryo

Figure 2.5: Distribution of Cl^- between whole egg, embryo, yolk sac, and tissue over the last 12 days of embryonic development. Means ± SE, n=5.

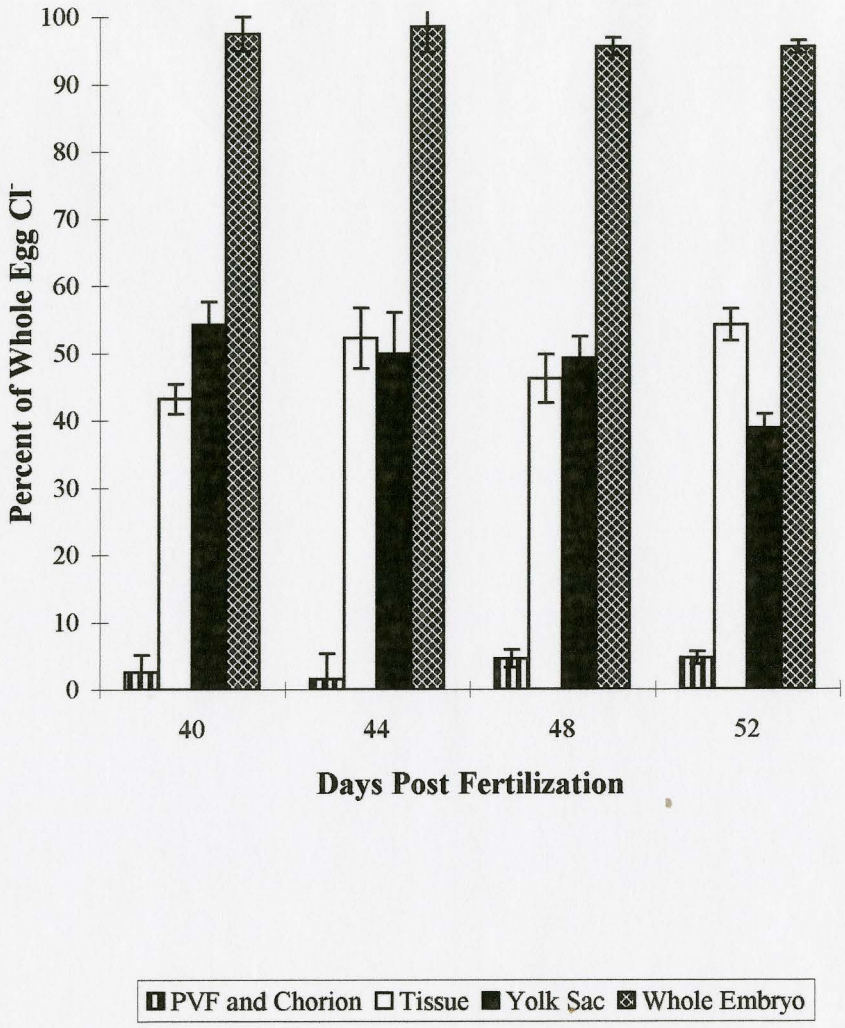
Percent of Whole Egg Cl-
100
90
80
70
60
50
40
30
20
10
0
40
44
48
52
Days Post Fertilization
PVF and Chorion
Tissue
Yolk Sac
Whole Embryo

Figure 2.6: Distribution of Ca^{2+} between whole egg, embryo, yolk sac, and tissue during the last 12 days of embryonic development.

Means $\pm$ SD, n = 5.

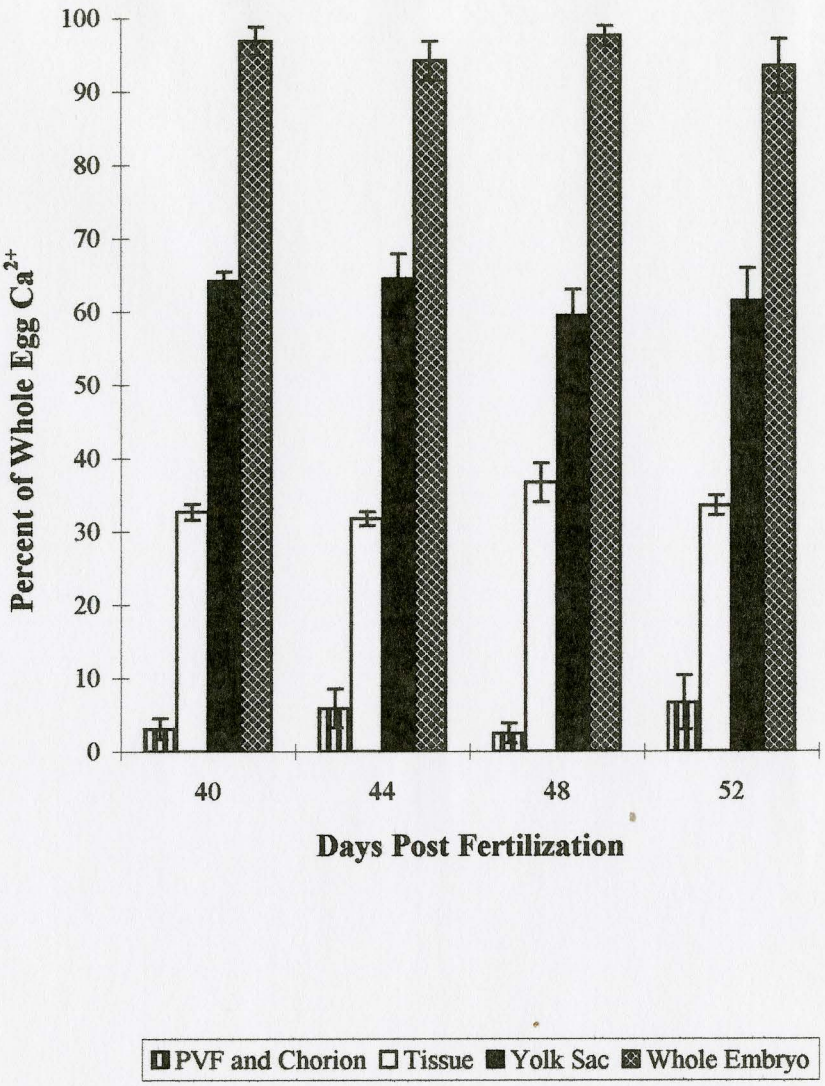
Percent of Whole Egg Ca^{2+}
100
90
80
70
60
50
40
30
20
10
0
40
44
48
52
Days Post Fertilization
PVF and Chorion
Tissue
Yolk Sac
Whole Embryo

Na^+ Uptake Kinetics

In both whole eggs and dechorionated embryos J_{in}^{Na+} (nEq $g^{-1}h^{-1}$) varied with external [Na^+]. In whole eggs, J_{in}^{Na+} was linearly related to external [Na^+] (day 31: $y=0.1x+5.6$; $R^2=0.9$; day 45: $y=0.1x+4.9$; $R^2=0.9$) (Figure 2.7 A). There was no evidence of saturation. By contrast, in dechorionated embryos, J_{in}^{Na+} was not related linearly to external [Na^+] (Figure 2.7 B). J_{max} decreased 2.2-fold and K_m decreased 5.5-fold between day 31 and day 45 (Table 2.4)

Ca^{2+} Uptake Kinetics

The Ca^{2+} uptake rate increased non-linearly with increasing external [Ca^{2+}] (Figure 2.8). J_{max} and K_m were both higher in whole eggs than in dechorionated embryos. Overall, J_{max} was 51.24- fold higher and K_m was 2.42- fold higher in whole eggs than in dechorionated embryos (Table 2.5).

J_{max} decreased 2.46- fold between day 28 and 42 in whole eggs and increased 1.3 fold in dechorionated embryos.

In whole eggs, K_m decreased 1.22- fold between day 28 and day 42. In dechorionated embryos, K_m dropped 2.48- fold between day 28 and 35, then increased 34-fold over the next 7 days.

Figure 2.7: The relationship between the Na^+ uptake rate ($nEq.g^{-1}h^{-1}$) and the external Na^+ concentration ($\mu mol.l^{-1}$) in **A**. whole eggs and **B**. dechorionated embryos at various stages of embryonic development. Means ± SE, n=5; temperature: 8°C.

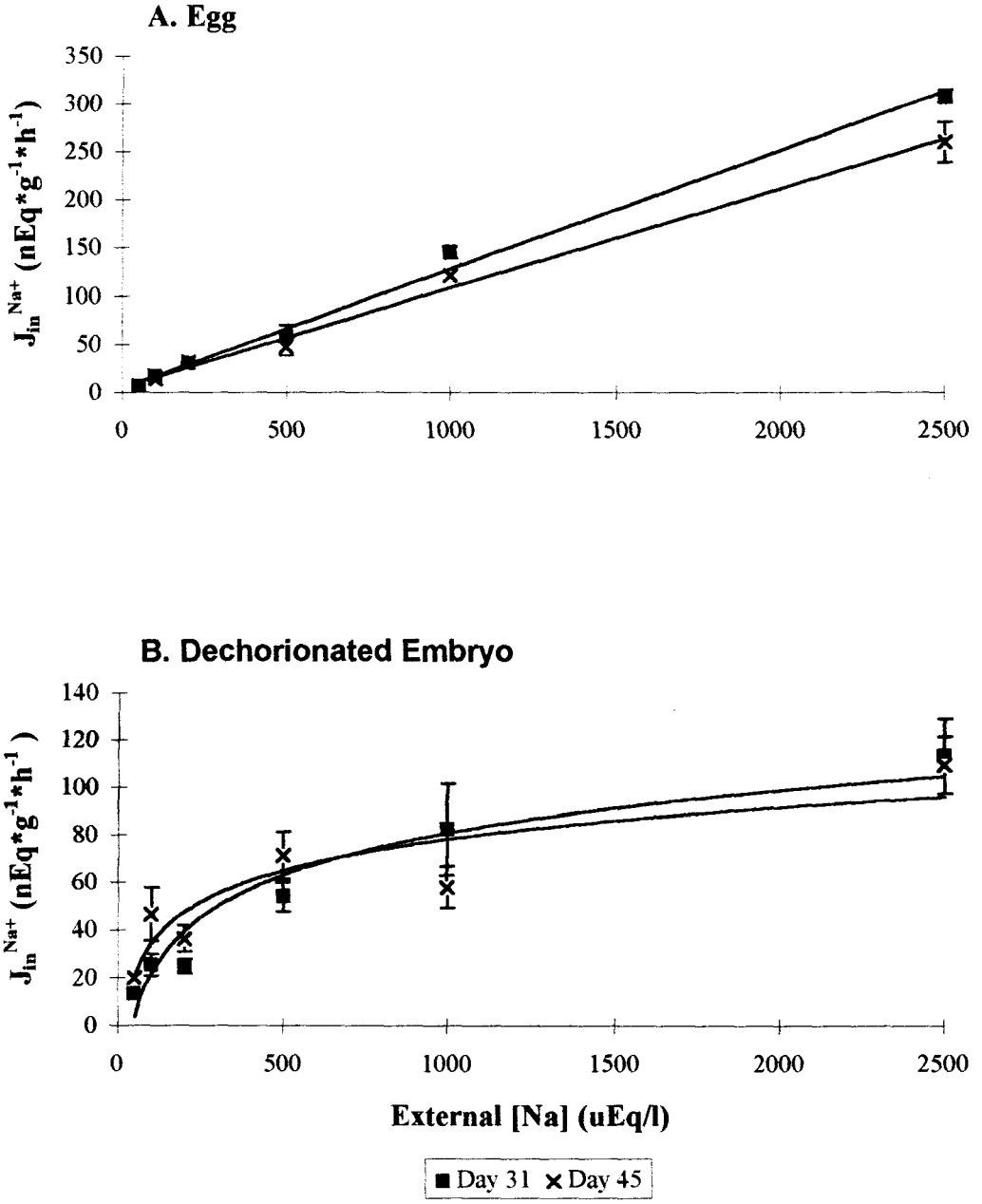
A. Egg
J_{in}^{Na+} (nEq*g^{-1}*h^{-1})
350
300
250
200
150
100
50
0
0
500
1000
1500
2000
2500
B. Dechorionated Embryo
J_{in}^{Na+} (nEq*g^{-1}*h^{-1})
140
120
100
80
60
40
20
0
0
500
1000
1500
2000
2500
External [Na] (uEq/l)
Day 31
Day 45

Table 2.4: Summary of K_m and J_{max} for $^{24}Na^+$ uptake kinetics in embryos over the last 14 days of embryonic development. Means ± SE, n=5.

Embryo Age (days after fertilization)	K_m ($mEq*l^{-1}$) ± SE	J_{max} ($\mu Eq*g^{-1}h^{-1}$)
Day 31	1.84 ± 0.05	0.27 ± 0.36
Day 45	0.33 ± 0.13	0.12 ± 0.01

Figure 2.8: The relationship between the Ca^{2+} uptake rate ($nEq.g^{-1}h^{-1}$) and the external Ca^{2+} concentration ($\mu mol.l^{-1}$) in **A**. whole eggs and **B**. dechorionated embryos at various stages of embryonic development.Means ± SE, n=5; temperature: 8°C.

A. Egg

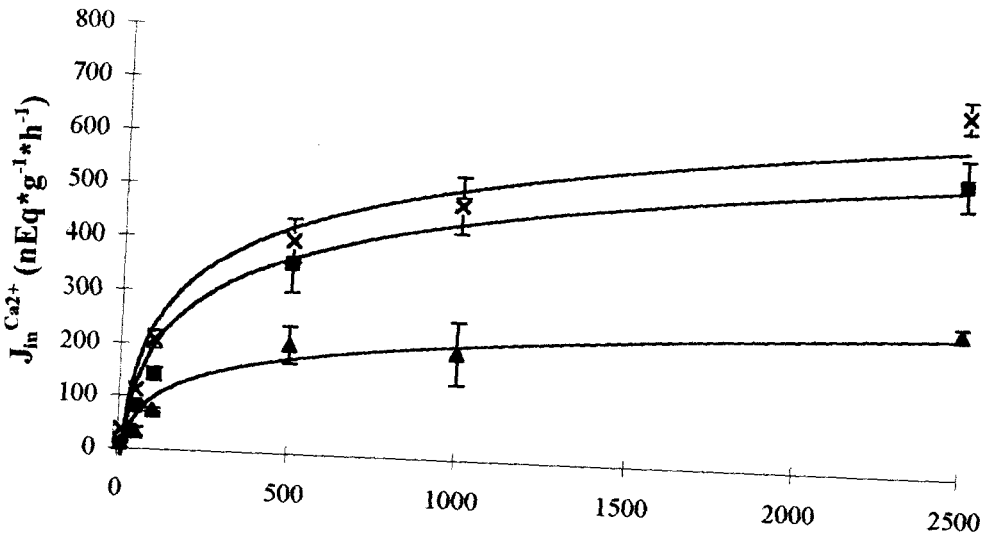

B. Dechorionated Embryo

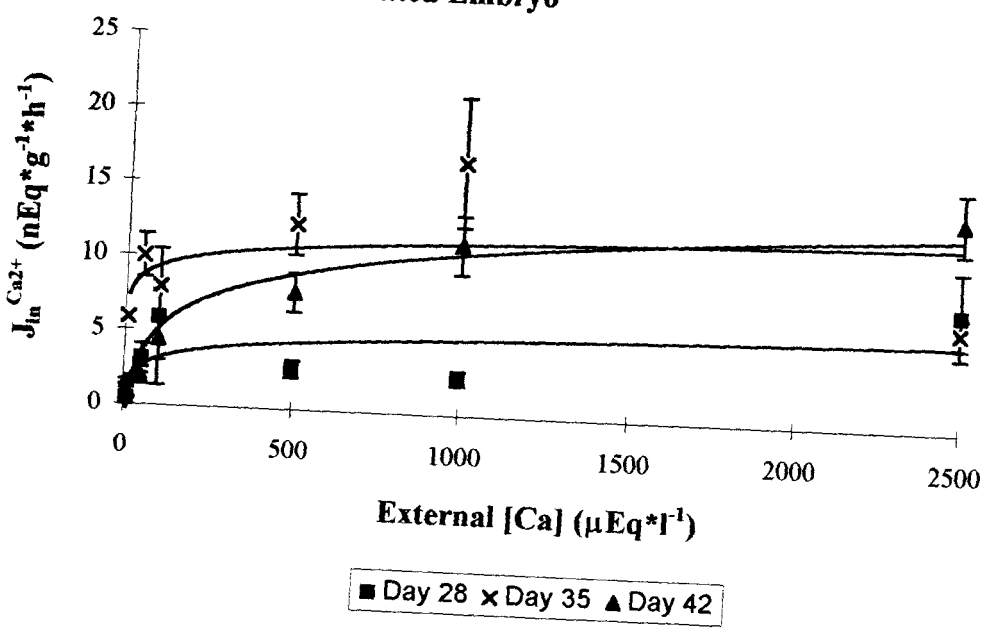

Table 2.5: Summary of K_m and J_{max} for $^{45}Ca^{2+}$ uptake kinetics in eggs and dechorionated embryos over the last 21 days of embryonic development. Means ± SE, n=5.

Egg/ Embryo Age (days after fertilization)	K_m ($mEq*l^{-1}$) ± SE	J_{max} ($nEq*g^{-1}*h^{-1}$) ± SE
Day 28- Egg	0.35 ± 0.026	0.63 ± 0.026
Day 28- Embryo	0.027 ± 0.047	0.0049 ± 0.002
Day 35- Egg	0.35 ± 0.11	0.72 ± 0.068
Day 35- Embryo	0.011 ± 0.015	0.012 ± 0.0022
Day 42- Egg	0.29 ± 0.084	0.29 ± 0.023
Day 42- Embryo	0.37 ± 0.12	0.016 ± 0.001

Na^+ Efflux in Whole Eggs and Dechorionated Embryos

Over the first 30 minutes of exposure to non- radiolabelled tap water, eggs lost 73.8% of their radioactivity, while dechorionated embryos lost 69.8%. After this period, further loss was negligible. The specific activity of the loading media was 141.2 and 147.5cpm/nEq for eggs and embryos, respectively.

The amount of exchangeable Na^+ during the 3 hour loading period was calculated using the following equations:

$$\textbf{Amount } {}^{24}\textbf{Na}^+ = \textbf{cpm / SA}$$

$$\textbf{\% Exchangeable Na}^+ = 100^* \textbf{ (Amount } {}^{24}\textbf{Na}^+ \textbf{ / Whole Egg or Embryo Na}^+ \textbf{ Content)}$$

where **amount $^{24}Na^+$** was the amount of radiolabelled Na^+ in the egg or embryo in nEq; **cpm** was the counts per minute per egg or embryo at the end of the 3 hour loading period in cpm; **SA** was the specific activity of the loading solution in cpm/ nEq; **% exchangeable Na^+** was the % of whole egg or embryo Na^+ exchanged with environment in the loading period; **whole egg Na^+ content** was the amount of Na^+ measured in whole eggs and embryos in nEq.

4.7% and 3.4% of whole egg and dechorionated embryo Na^+, respectively, was exchangeable in 3 hours.

Ca^{+} Efflux in Whole Eggs and Dechorionated Embryos

Over the first 30 minutes of exposure to non- radiolabelled tap water, eggs lost 97.55% of their radioactivity, while dechorionated embryos lost 36.0%. After 30 minutes, neither the eggs nor the embryos lost significant amounts of $^{45}Ca^{2+}$. The specific activity of the loading media was 259.81 and 294.74 cpm/nEq for eggs and embryos, respectively.

Using the equations above and the whole egg and embryo Ca^{2+} content, it was found that eggs exchanged 5.72% of their whole egg Ca^{2+} in 3 hours. However, dechorionated embryos exchanged only 0.12% of their whole body Ca^{2+} over the same period.

DISCUSSION

Whole Egg Water Content

The results show that whole egg water content, wet weight, and dry weight do not change from the time of fertilization to the time of hatch (Table 2.2). Whole eggs had a water content of 64.4% whole egg wet weight throughout embryonic development. Kamler (1992) argued that when freshly spawned *O. mykiss* eggs are shed into fresh water, they absorb approximately 27% of their initial water volume in 30 minutes. She suggested that after termination of swelling, there is no further change in water content until after hatch. In addition, Kamler (1992) suggested that although whole egg weight is influenced by environmental factors such as O_2 availability, it is determined primarily by genetic factors.

The present water content findings are similar to those of previous studies. *O. mykiss* eggs were found to have a water content between 55.6 and 65.0% whole egg wet weight (Kamler, 1992). Similarly, Atlantic salmon eggs (*Salmo salar*) had a water content of 67.21% (Eddy and Talbot, 1985). Also, *Salmo gairdneri* had water content of 65.5% in distilled water, 63.6% in 11% sea water and 63.9% in 13% sea water (Shen and Leatherland, 1977).

Throughout embryonic development, the yolk sac comprised the greatest proportion of whole egg wet weight (Figure 2.2). Although this tissue has a low water content (only 52.96% water, compared to the embryonic tissue which is approximately

87.29% water- Eddy and Talbot, 1985), it is the largest energy source for embryos and larvae prior to exogenous feeding. This yolk sac is utilized by the embryos and larvae until it is exhausted at approximately 250dd, when exogenous feeding begins (Misiaszek, 1996).

Growth in a developing embryo is characterized by an increase in body size over a short period of time (Kamler, 1992). In the present experiment it was determined that over the last 12 days of development there was a 1.9-fold increase in wet weight in embryonic tissue (yolk sac removed). One day prior to hatch, yolk sac-free embryos comprised 13.02% of whole egg wet weight. This agrees well with a previous study in which yolk sac-free Atlantic salmon embryos were found to comprise 14.7% of the whole egg wet weight (Eddy and Talbot, 1985). During this time, the embryo is elaborating tissue and developing major organ systems (Blaxter, 1969).

Whole Egg Ion Content and Distribution

Until just prior to hatching, Na^+ was the least abundant electrolyte of those studied in whole rainbow trout eggs (Figure 2.3). Its linear relationship with dry weight (Figure 2.2) suggests that whole egg ion content is determined largely by genetic factors and maternal contribution (Misiaszek, 1996). Despite the low inital levels of Na^+, significant rates of accumulation were recorded over the last 20 days of embryonic development in all lots tested. This suggests that whole eggs are capable of regulating their Na^+ levels and that they may posess a mechanism for taking up Na^+ from the environment prior to hatching.

There was also evidence that embryos are capable of taking up Na^+ from the yolk sac, pvf, or both during embryonic development. Figure 2.4 suggests that both whole embryos and yolk sac-free embryos show a significant increase in Na^+ content over the last 12 days of embryonic development. The lack of a change in yolk sac Na^+ content over the same period suggests that the embryo may be gaining Na^+ from the pvf.

The results of the present study are similar to those of other studies. This study is unique, however, in that it has combined changes in ion content with changes in ion distribution in *O. mykiss* throughout much of embryonic development. Despite the inherent differences in experimental methods between studies, results of other experiments can be compared to the present study. For example, it has been shown in both *Salmo salar* and *Salmo gairdneri* that Na^+ content increases through embryonic development (Rudy and Potts, 1969; Shen and Leatherland, 1977). Similarly, the distribution of Na^+ found in eggs of *O. mykiss* in the present study was very similar to that found by Eddy and Talbot (1985) in eggs of Atlantic salmon (In *O. mykiss*, 93.1% whole egg Na^+ was in whole embryo and 6% was in pvf and chorion; In Atlantic salmon, 93.6% whole egg Na^+ was in whole embryo and 10.6% was in pvf and chorion).

Ca^{2+} was the most abundant electrolyte of those studied (Figure 2.3). As was the case with Na^+, the amount of whole egg Ca^{2+} was linearly related to dry weight (Figure 2.2), suggesting maternal contribution to initial egg electrolyte level. The possibility of net Ca^{2+} accumulation in eggs was not clear in the present investigation. Although significant accumulation was found in 2 of the 4 lots sampled, the remaining lots showed a net loss or no change in Ca^{2+} content (Table 2.3). The lack of clear evidence for Ca^{2+} accumulation

does not necessarily mean that eggs are not capable of regulating it prior to hatch. It may suggest that if Ca^{2+} transport mechanisms exist in eggs and embryos, they may either be underdeveloped or not used for ion regulation at this stage

Perhaps embryos do not require high levels of the ion until after hatching, when Ca^{2+} is used for skeletal ossification and bone mineralization (Steingraeber and Gingerich, 1991). Since neither the distribution within eggs nor the content of Ca^{2+} within whole embryos, yolk sac-free embryos and pvf change during the last 12 days of embryonic development (Figure 2.6), it is possible that the embryo and yolk sac contain all the required Ca^{2+} upon fertilization.

It is also possible that if maternal contribution of Ca^{2+} is insufficient to meet the demands of the developing embryo, exogenous supplies of Ca^{2+} may be taken up by the embryo. This may explain why two of the four lots sampled showed a net accumulation of Ca^{2+}, while the other two lots showed no change. To provide evidence for this, it would be necessary to alter the maternal [Ca^{2+}] so as to determine the effects of low maternal contribution to ion levels.

Although evidence for Ca^{2+} regulation in embryonic and larval teleosts is very limited, it is clear for some species that until sometime after hatching, embryos and larvae utilize the Ca^{2+} stores within their yolk sacs until a critical yolk sac weight is acheived (Hwang *et al.*, 1994; Misiaszek, 1996; Peterson and Martinrobichaud, 1986). In the current study, yolk sacs represent the largest source of Ca^{2+} within the egg.

Cl^- is less abundant than Ca^{2+} but more abundant than Na^+ in whole eggs at the beginning of embryonic development (Figure 2.3). However, by the end of embryonic

development, eggs have virtually equal amounts of Na^+ and Cl^-. Maternal contribution to initial whole egg ion content was also evident by the linear relationship between Cl^- content and dry weight (Figure 2.2). As was the case with Ca^{2+}, the results of the present study are not clear as to whether or not a significant accumulation of Cl^- occurs in eggs prior to hatching. Accumulation rates were only significant in half of the lots measured (Table 2.3). Again, it is possible that if maternal contribution of Cl^- is not sufficient, embryos may take up the anion from the pvf or environment. These findings do not discount the possibility of Cl^- regulation by eggs.

Interestingly, there was a significant increase in Cl^- content in the embryonic tissue over the last 12 days of development (Figure 2.5). At the same time, yolk sac Cl^- levels dropped significantly. This may suggest that even if eggs are not gaining net amounts of Cl^-, the developing embryo is capable of taking up Cl^-, possibly from the yolk sac.

Na^+ Uptake Kinetics

In whole eggs, the rate of $^{24}Na^+$ uptake was linearly related to external $[Na^+]$ (Figure 2.7). This suggests that Na^+ enters the egg via diffusion across the chorion into the pvf. However, in dechorionated embryos, there was a non-linear relationship between external concentration of Na^+ and the rate of Na^+ uptake (J_{in}^{Na+}). Na^+ uptake displayed typical Michaelis-Mentin kinetics. Up to a certain point (J_{max}), Na^+ uptake by the animal was dependent on the external concentration of the ion. Beyond that point, further increases in external concentration had no effect on Na^+ uptake. The evidence for saturable Na^+ uptake in dechorionated embryos suggests that there may be selective

transporting cells at the surface of the embryo. There is evidence for the presence of specific ion transporting cells in the yolk sac, pericardial, cutaneous, and branchial epithelia of freshwater teleosts prior to hatching (Li *et al.*, 1995; Ayson *et al.* 1994; Hwang *et al.*, 1994; Alderdice, 1988; Hwang and Hirano, 1985). The saturable nature of $^{24}Na^+$ uptake by dechorionated embryos does not necessarily mean that active uptake is occurring; facillitated diffusion is also saturable and it does not require energy.

J_{max} is related to the affinity of a transport carrier or selective channel (K_m). A high K_m indicates a low affinity of the carrier or channel for the ion (McWilliams and Shephard, 1989). The results of this study showed that K_m decreased in dechorionated embryos between day 31 and 45 (Table 2.4). This suggests that the embryo has ion transporting cells which increase their affinity for Na^+ just prior to hatching. These ion transporting cells are possibly chloride cells, as described previously for numerous teleost species (Misiaszek, 1996; Shen and Leatherland, 1977; Alderdice, 1988; Hwang, 1989; Kaneko *et al.*, 1995; Hwang *et al.*, 1994; Ayson *et al.*, 1994, 1995).

First day rainbow trout hatchlings were shown to have a very low K_m for Na^+ (Misiaszek, 1996). This agrees well with results of the present experiment. Misaszek (1996) argued that since there is such early evidence of transporting cells, it is possible that they play a role other than ion balance. She argued that they may play a role in acid-base regulation, perhaps by Na^+/H^+ exchange. This may also be the case with embryos, although further investigations must be done before it can be proven.

The magnitude of J_{max} depends on the transporting surface area, the number of Na^+ transporting cells, the number of Na^+ channels in the transporting cells, or any combination

of the three (Misaszek, 1996). The fact that the dechorionated embryos are capable of taking up radiolabelled Na^+ suggests that the surface of the embryo contains the appropriate transporting cells prior to hatching.

J_{max} decreased in dechorionated embryos between day 31 and 45 (Table 2.4). This was not expected, since the gill and cutaneous surfaces elaborate prior to hatch, providing a larger surface area across which ions may be transported (Rombough, 1988, Morgan, 1974; Wells and Pinder, 1996). Rombough (1988, 1991) argued that the cutaneous surfaces of embryonic and larval teleosts such as rainbow trout have a large surface area and thus act as the primary respiratory and ion exchange surface before the gills develop. However, it is possible that the ability to take up ions, such as Na^+, is temporarily hindered shortly before hatching because of the activity and energy required by the embryo to free itself from the chorion.

The Na^+ efflux experiment performed in the present study showed that losses of ion occurred in both whole eggs and dechorionated embryos. In both cases, losses were rapid in the first 30 minutes, then were very slow for the remainder of the experiment. In a similar experiment with Atlantic Salmon, Eddy and Talbot (1985) argued that although eggs and dechorionated embryos lose Na^+ very rapidly within the first few minutes of the experiment, they lose Na^+ very slowly after that. They suggested that even after 13 days, each egg only exchanged 19% of its whole egg Na^+.

In the 3 hour loading period, the amount of exchangeable Na^+ was found to be 4.7% and 3.4% of whole egg and embryo Na^+, respectively. The similarity of Na^+ exchangeabilities suggests that prior to hatching, rainbow trout embryos are capable of

taking ions from the environment, whether it be pvf or external water. The slightly lower Na^+ exchangeability in dechorionated embryos may show that transport mechanisms are not fully developed until after hatching. The fact that whole eggs exchange 4.7% of their whole egg Na^+ content in 3 hours is interesting because this study has also shown that 7% of whole egg Na^+ was found in the pvf and chorion at 52 days post fertilization (figure 2.4). The fact that exchangeable Na^+ nearly equals pvf and chorion Na^+ content suggests that the Na^+ that is being exchanged is from the pvf, chorion, or both. These findings are similar to those of Eddy and Talbot (1985) and Rudy and Potts (1969) which showed that accessible Na^+ space (contains readily exchangeable Na^+) in Atlantic Salmon was similar to the volume of pvf and chorion.

Ca^{2+} Uptake Kinetics

Ca^{2+} uptake by whole eggs and dechorionated embryos also showed saturable Michaelis-Mentin kinetics (Figure 2.8). K_m and J_{max} were much greater in whole eggs than in dechorionated embryos (Table 2.5).

K_m was much higher in whole eggs than in dechorionated embryos. In addition, K_m decreased in both eggs and embryos over the last 14 days of embryonic development. This reflects a much higher affinity of transporters or channels on the surface of the embryo than those on the chorion and also a higher affinity of the transporting mechanism as hatching approaches. Since the chorion is an acellular material, it is unlikely that special transporting cells would be present. It is likely, however, that ion channels or pores cover the surface of the chorion (Peterson and Martinrobichuad, 1986, 1993).

The large increase in K_m in dechorionated embryos between day 35 and 42 indicates a drop in transporter affinity for Ca^{2+} over this period. This may be due to activities and processes associated with hatching which would interfere with ion uptake.

Dechorionated embryos do not appear to take up large amounts of Ca^{+} (low J_{max}, Table 2.5) prior to hatching. This is in accordance with data for rainbow trout hatchlings, which showed that until approximately 200dd after hatching, larvae do not take up significant amounts of Ca^{2+} from the environment. They utilize only Ca^{2+} stored within their yolk sacs (Misiaszek, 1996). The J_{max} decreased in whole eggs as development proceeded, suggesting that as hatching approached, the chorion may have been damaged by the hatching enzyme (Steingraeber and Gingerich, 1991). This would allow some of the pvf to leak out of the egg, thereby causing a loss of ions and possibly a disruption of the permeability characteristics of the chorion.

In whole eggs and dechorionated embryos, respectively, 5.72% and 0.12% of whole egg and embryo Ca^{2+} was exchangeable. The pvf and chorion contain approximately 5% of whole egg Ca^{2+} (Figure 2.6), suggesting that the Ca^{2+} that is being exchanged is from the pvf or chorion or both. The very low amount of exchangeable Ca^{2+} in dechorionated embryos supports the suggestion that prior to exogenous feeding, embryos and larvae do not take Ca^{+} from the environment.

Conclusions

- Wet weight and water content of whole eggs do not change throughout embryonic development.

- Accumulation of Na^+, Ca^{2+}, and Cl^- was measured in whole eggs, suggesting an ability of embryos to ionoregulate.
- Redistribution of Na^+ and Cl^- occurs between the yolk sac and body tissue. There are no changes in Ca^{2+} distribution prior to hatching.
- Na^+ uptake by whole eggs is non-saturable, suggesting that diffusion of Na^+ occurs across the chorion into the pvf.
- Na^+ uptake in dechorionated embryos is saturable, suggesting an active uptake or facilitated diffusion mechanism at the surface of embryos.
- Ca^{2+} uptake by whole eggs and dechorionated embryos is saturable, suggesting an active uptake or faciliated diffusion mechanism at the surface of the embryo.
- Very low Ca^{2+} uptake rates in dechorionated embryos suggest that the Ca^{2+} uptake mechanism is not fully developed until after hatching.

CHAPTER 3: UNSTIRRED LAYERS AND LOCALIZATION OF ION ACTIVITY IN EMBRYONIC RAINBOW TROUT

INTRODUCTION

Eggs and embryos of salmonids, such as rainbow trout (*O. mykiss*) are metabolically active prior to hatching (Rombough, 1988; Boulekebache, 1981). This means that embryos are taking up O_2 and are presumably excreting CO_2 and NH_3/NH_4^+ (Rombough, 1998; Rombough, 1988; Rombough and Ure, 1991; Wright *et al*, 1995; Rahaman-Norohna *et al*, 1996). These materials are taken up from and excreted into the unstirred layer (USL) of water adjacent to the animal. An unstirred layer is a region of semistagnant water adjacent to an organism where oxygen is depleted and metabolic wastes accumulate (Rombough, 1988).

In adult teleosts, rates of CO_2 excretion are 10 times those of NH_3 excretion and many more times those of H^+ excretion (Randall and Wright, 1989). As CO_2 is excreted it combines with water to form HCO_3^- and H^+, the latter of which acidifies the water adjacent to the gills (Randall and Wright, 1989). The reaction is catalysed by carbonic anhydrase which is found in mucous at the surface of the gills. Protons from this reaction combine with excreted NH_3 to form NH_4^+ (Randall and Wright, 1989).

NH_3 excretion is primarily via NH_3 movement down its P_{NH3} gradient (Randall and Wright, 1989; Wright, 1995). The pK of the protonation of NH_3 to NH_4^+ is approximately 9.5 (Randall and Wright, 1989). As a result, in most aquatic environments,

the majority of the NH_3 excreted will form NH_4^+, and thus will maintain a favorable P_{NH3} gradient between body fluids and the environment.

Very few studies have investigated the extent of USL acidification around teleost eggs and how this is related to NH_3/NH_4^+ excretion (Rahaman-Norohna *et al.*, 1996). The sites of production of NH_3/NH_4^+ are unknown, as are the locations of excretion. In addition, the extent of CO_2 excretion has never been measured adjacent to embryos.

Conventional methods of determining the extent of excretion of products such as NH_3, NH_4^+, and CO_2 are not particularly useful for use in embryonic teleosts. Not only are they not sensitive enough to measure the small changes in ion concentration, but they are also not able to provide information on the specific location of excretion of these materials at the surface of embryos.

Ion selective microelectrodes (ISMEs) provide a relatively simple method of measuring small changes in concentration of ions such as H^+ and NH_4^+ in the USL of small organisms and tissues (Ammann, 1986; Rahaman-Norohna *et al*, 1996; Collier and O'Donnell, 1997; Misiaszek, 1996). Measuring concentration differences at various locations adjacent to an organism provides an indication of specific sites of ion excretion. If there are no differences in ion concentration measured at various locations adjacent to an organism, it is likely that all body surfaces contribute equally to the excretion of those ions.

Recently, ISMEs have been used to determine the extent of oxygen uptake across various epithelia of Atlantic salmon larvae (Rombough, 1998). In addition, an ISME method for the simultaneous measurement of pH and P_{CO2} has been described for use in

tissue preparations (Voipio and Ballanyi, 1997; Bomsztyk and Calalb, 1986). This method has never been attempted for live, whole animal preparations.

It is the purpose of this chapter to determine if acidification and NH_4^+ and CO_2 accumulation occurs at the surface of rainbow trout eggs and embryos. Using ISMEs, $[H^+]$, $[NH_4^+]$, and P_{CO2} are measured at various locations adjacent to eggs and dechorionated embryos and at various stages of embryonic development. The possible roles of pvf and chorion in the excretion of these materials will also be discussed.

MATERIALS AND METHODS

Experimental Animals

Rainbow trout eggs were obtained and maintained as described in Chapter 2.

Ion-Selective Microelectrodes and Data Acquisition

Ion selective microelectrodes (ISME) were used to measure pH and specific ion concentrations at various locations around rainbow trout eggs and embryos. ISMEs were made from double-barrel non-filamented glass capillary tubes (World Precision Instruments Inc.) following a method similar to that described by O'Donnell (1992). The glass was silanized to help prevent the experimental water from entering the tip and displacing the hydrophobic ionophore cocktail. Prior to silanization, the glass was soaked in concentrated nitric acid for 5 minutes, rinsed briefly in H_2O_{dd} and dried on a heating plate in a fume hood. Each ISME was placed in a vertical micropipette puller (Narishige), pulled to a tip diameter of <1μm and placed on a heating plate at 200°C. Dimethyldichlorosilane or trimethyldimethylsilylamine (approximately 2ml) (Sigma) was placed in a petri dish which was inverted over the ISMEs on a heating plate for 10 minutes. Electrodes were placed in a dessicator until use. In all experiments, reference electrodes were unsilanized filamented 1mm single-barrel glass capillary tubes (World Precision Instruments Inc.) filled with 3 M KCl.

Each barrel of the electrode was connected to a pH/ion amplifier (Model 2000, A-M Systems) using $AgCl_3$ coated silver wire. The signal was fed through an analog to digital

converter (TL1 DMA Interface, Axon Instruments), then displayed and recorded on a PC-based data acquisition system (AXOTAPE, Axon Instruments, Burlingame, California).

Localization of NH_4^+ and pH Differences

Double-barrel ISMEs were used for simultaneous measurement of [NH_4^+] and pH around eggs and dechorionated embryos at various stages of late embryonic and early larval development. The tips of the electrodes were broken slightly (<20μm) to reduce electrode resistance and noise.

The tip and shank of one barrel was filled with a pH ionophore cocktail based on the neutral carrier tridodecylamine (H^+ ionophore cocktail B, 95293 Fluka). The remainder of the barrel was backfilled with a solution containing 100μM NaCl and 100μM sodium citrate, pH 6.0.

The tip and shank of the other barrel was injected with an NH_4^+ ionophore containing 7.5% nonactin, 2.5% monactin, 1% sodium tetraphenylborate, and 89% nitrophenyloctylether (Fluka). The remainder of the barrel was backfilled with a solution of 500 mmol/l NH_4Cl.

The pH barrel was calibrated using 2 solutions similar in ionic strength to the experimental bath water. The solutions were titrated with NaOH or HCl until they differed by 1 pH unit. A pH macroelectrode, calibrated with standard solutions of pH 4 and 7, was used to monitor the pH of the calibration solutions for each experiment.

The NH_4^+ barrel was calibrated with 3 solutions containing 1, 10, and 100μmol/l NH_4Cl in bath water (pH was adjusted to 8.0 with 1N NaOH). Due to significant levels of

ammonia (approximately 5-10μmol/l) in the water used to make the calibration solutions and bath water, it was necessary to remove the ammonia from the water by passing H_2O_{dd} through Dowex-50 ion exchange resin (Sigma, 50X8-W). Dowex-50 was subsequently removed by vacuum filtration. Bath water was made by adding 1.0mmol/l NaCl, 0.5mmol/l $CaCl_2$, and 0.5mmol/l Na_2CO_3 to the ammonia-free water and adjusting pH to 8.0 with NaOH.

Thirty minutes prior to each experiment, eggs were chosen at random from their holding containers. Half of the eggs were dechorionated and all animals were maintained in 7°C dechlorinated tap water in subdued light until use. Embryos were exposed briefly to 0.06g/L MS222 in bath water (pH 8.0), which induced light anaesthesia for approximately 30 minutes. It was necessary to anaesthetize the dechorionated embryos prior to each experiment because excessive movements of embryos damaged the electrodes. Whole eggs did not require anaesthetic. Immediately before each experiment, anaesthetized animals were rinsed briefly in bath water to remove surface-bound MS222. Each egg and embryo was placed in a bath water-filled petri dish containing a layer of Sylgard. Small pins were embedded in the Sylgard to confine the dechorionated embryos to a small area for the duration of the experiment.

For each measurement, an ISME was placed 10-20μm away from the surface of eggs and dechorionated embryos. A dissecting microscope (16-40x magnification) was used to observe the position of the electrode and a micromanipulator was used to move the electrode to appropriate positions. Measurements were made at locations around the chorion, gills, yolk sac and trunk (i.e. developing embryo excluding yolk sac) (Figure 3.1). Preliminary measurements made at different locations around whole eggs showed that there were no differences in pH or $[NH_4^+]$ between these sites. As a result, subsequent measurements were

Figure 3.1: Locations of NH_4^+ and pH measurements around the dechorionated embryo using ISMEs. P_{CO2} was measured only at the surface of the gills.

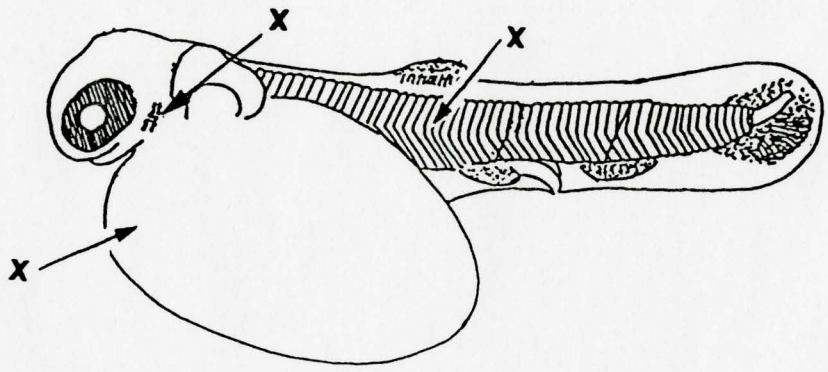
X
X
X

made at a single location adjacent to the eggs. After each measurement, a bulk water measurement was taken greater than 1cm from the specimen. In all cases, potentials were measured relative to a reference electrode filled with 3M KCl which was positioned greater than 1cm away from the eggs and embryos.

At the end of each experiment, all animals were monitored to ensure complete recovery. Results from embryos which failed to recover from anaesthesia were discarded.

The pH of the bath water and of the USL next to the surface of eggs and dechorionated embryos was determined using the following equation:

$$\mathbf{pH = pH_{cal} - (\Delta mV/S)}$$

Where, $\mathbf{pH_{cal}}$= pH from one of the calibration solutions
ΔmV= difference between calibration pH reading and bath water or USL pH reading (mV)
S= slope of pH electrode for a 1pH unit change

The ammonium concentration of the bath water and of the water next to the surface of the egg or dechorionated embryo (in μM) was calculated using the following equation:

$$\mathbf{[NH_4^+] = [NH_4^+]_{cal} * 10\text{^}(\Delta mV/S)}$$

Where, $\mathbf{[NH_4^+]_{cal}}$= concentration of ammonium from an NH_4^+ calibration solution (μM)
ΔmV= difference (in mV) recorded when the electrode was moved between the calibration solution and the bulk water or USL
S= slope of the NH_4^+ electrode for a 10- fold change in $[NH_4^+]$ (mV)

pH and P_{CO2} Around Whole Eggs and Dechorionated Embryos

A modified ISME technique was used for simultaneous measurements of pH and P_{CO2} in the USL of dechorionated embryos. As described by Bomsztyk and Calalb (1986), Voipio and Kaila (1993), and Voipio and Ballanyi (1997), this method has a significantly faster response than previous P_{CO2} microelectrodes. A double-barrel ISME was used in which one barrel was sensitive to P_{CO2} and both barrels were sensitive to pH. P_{CO2} was then calculated by subtraction.

Silanized double-barrel capillary glass was pulled to a tip diameter of <1μm and broken back to a diameter of 4-10μm. One barrel, to become CO_2 sensitive, was first backfilled up to the shank with a solution containing 150mM NaCl and 1 mg/ml carbonic anhydrase (Sigma). NaOH was added to yield a pH higher than 9.0.

The filling solution for the H^+- selective barrel was 100μM NaCl and 100μM Na citrate, pH 6.0. Pressure was applied by syringe to force out air in the shank and tip. The tip was then immersed in a liquid membrane solution (H+ ionophore cocktail 1, I-37772 Sigma). Care was taken to ensure the ionophore cocktail was saturated with 100% CO_2 prior to use. If the cocktail was not CO_2 saturated, the electrode did not respond to changes in external P_{CO2}.

Slight suction was applied by syringe to the pH barrel (i.e. the barrel containing NaCl and Na citrate), so as to take up a column of ionophore cocktail about 300 μm in length. A brief pulse of weak suction was then used to take up a very short column (≤20 μm) of the

ionophore into the tip of the other barrel containing NaCl and carbonic anhydrase. This barrel will thus be sensitive to changes in both pH and P_{CO2}.

P_{CO2} was calculated as the difference in the signals of the two barrels:

$$\mathbf{P_{CO2} = pH - (P_{CO2} + pH)}$$

where $\mathbf{P_{CO2}}$ equals the change in potential in the P_{CO2} barrel after subtraction; **pH** equals the change in potential from the pH barrel; $\mathbf{(P_{CO2} + pH)}$ equals the gross change in potential in the P_{CO2}/ pH sensitive barrel prior to subtraction of the pH potential.

The signal was calculated in this way (i.e. inverted) so that increases in external P_{CO2} result in a positive-going change in electrode potential. CO_2 diffuses across the short column of ionophore cocktail, is hydrated to produce H^+ and HCO_3^- by the action of carbonic anhydrase, and acidifies the backfill solution in the inner interface of the cocktail. Electrode potential thus shifts negative (i.e. the same direction as when the external pH is made more basic). In effect, an increase in P_{CO2} drives the electrode response negative and subtraction is done as above so that an increase in P_{CO2} moves the potential in the same direction as an increase in $[H^+]$.

Electrodes were calibrated using step changes in P_{CO2} (at constant solution pH) and changes in solution pH (at constant P_{CO2}). The pH electrode was calibrated with two samples of bath water (dechlorinated Hamilton tap water with 3mmol/l NaCl, titrated to pH 8.9 with 1N NaOH) differing by 1 pH unit. The P_{CO2} barrel was calibrated with bath water equilibrated with either 2% or 9% CO_2 (balance O_2). Taking into consideration water vapour pressure at

20°C, the corresponding P_{CO2} values were 14.8 and 66.8mmHg, respectively. Bicarbonate was added to each P_{CO2} calibration solution to maintain solution pH. Bicarbonate levels in the 2% and 9% CO_2 solutions, calculated using the Henderson- Hasslebalch equation, were 10.7mmol/l (0.9g/l) and 48.8mmol/l (4.1g/l), respectively. The calibrations were done at the same temperature as the experiments (7- 12°C).

After the electrodes were assembled and calibrated, measurements of pH and P_{CO2} were made at the surface of the gills in dechorionated embryos. Electrodes were positioned with a micromanipulator and were observed with a 16-40x dissecting microscope. The electrode was placed 10-20μm from the surface of the embryo. The reference electrode (3M KCl) was placed greater than 1cm away from the surface of the animals.

The CO_2 calibration solutions had less than a ten-fold difference between them (14.8 and 66.8 mmHg). A corrected slope corresponding to the change in potential for a 10-fold change in P_{CO2} was therefore determined using the following equation:

$$S=\Delta_1 / \log (P_{CO2(1)} / P_{CO2(2)})$$

Where, S= corrected slope representing a 10-fold change in PCO_2
Δ_1= change in mV between two calibration solutions
$P_{CO2(1)}$= highest calibration P_{CO2}
$P_{CO2(2)}$= lowest calibration P_{CO2}

The unknown PCO_2 was then calculated using the following equation:

$$P_{CO2}\text{ (bath water or USL)} = P_{CO2\,cal} * 10\text{^}(\Delta_2/S)$$

Where, $P_{CO2\,cal}$= one calibration value for CO_2 (mmHg)

Δ_2= the change in mV between one P_{CO2} calibration solution and experimental (bath water or USL) measurement.

Statistical Analysis

Differences between 2 means were compared using student t-tests. Differences between more than 2 means (i.e. changes in pH different ages or in pH differences at different sites) were analysed using either one-way or two-way analysis of variance (ANOVA). Tukey and least standard difference (LSD) post-hoc tests were then performed to determine significance between variables. Differences were judged to be significant if $p < 0.05$.

RESULTS

pH Around Egg and Dechorionated Embryo

At all ages, the pH of the unstirred layer (USL) around eggs was more acid than the bulk water (t-test, $p<0.05$) (Figure 3.2). The mean pH of the USL around whole eggs ranged from 0.20 ± 0.01 to 0.60 ± 0.05 units acid relative to the bulk water between 15 and 42 days after fertilization. This represents a range of $[H^+]$ between 2.6 ± 4.2nmol/l and 68.7 ± 6.9nmol/l. There was a significant increase in acidity of whole egg USL between day 30 and 38 (ANOVA, $p<0.05$), followed by a significant decline between day 38 and 42 (ANOVA, $p<0.05$).

pH in the USL of dechorionated embryos was also acid relative to the bulk water at all ages (t-test, $p<0.05$) (Figure 3.3). Acidification was greater around the gills (0.41 ± 0.05 to 0.81 ± 0.06 units acid relative to bath water) and trunk surface (0.48 ± 0.11 to 0.72 ± 0.05 units) than around the yolk sac (0.29 ± 0.94 to 0.67 ± 0.25 units) from 25 to 51 days after fertilization (ANOVA, $p<0.05$).

In the USL around both the gills and yolk sac, there was a small but significant drop in acidification between day 25 and 35 (gills change from 0.81 to 0.41; yolk sac changes from 0.47 to 0.29 units acid relative to bulk water). This was followed by a significant increase in acidification around gills between day 38 and 42 (0.41 to 0.63 units acid relative to bath water) (ANOVA, $p<0.05$). The USL adjacent to the trunk surfaces

Figure 3.2: Changes in acidification of the unstirred layer around whole eggs at different stages of embryonic development, relative to bath water. Arrow indicates day of hatching. Bath pH is 7.9.

Means ± SE, n=4-5.

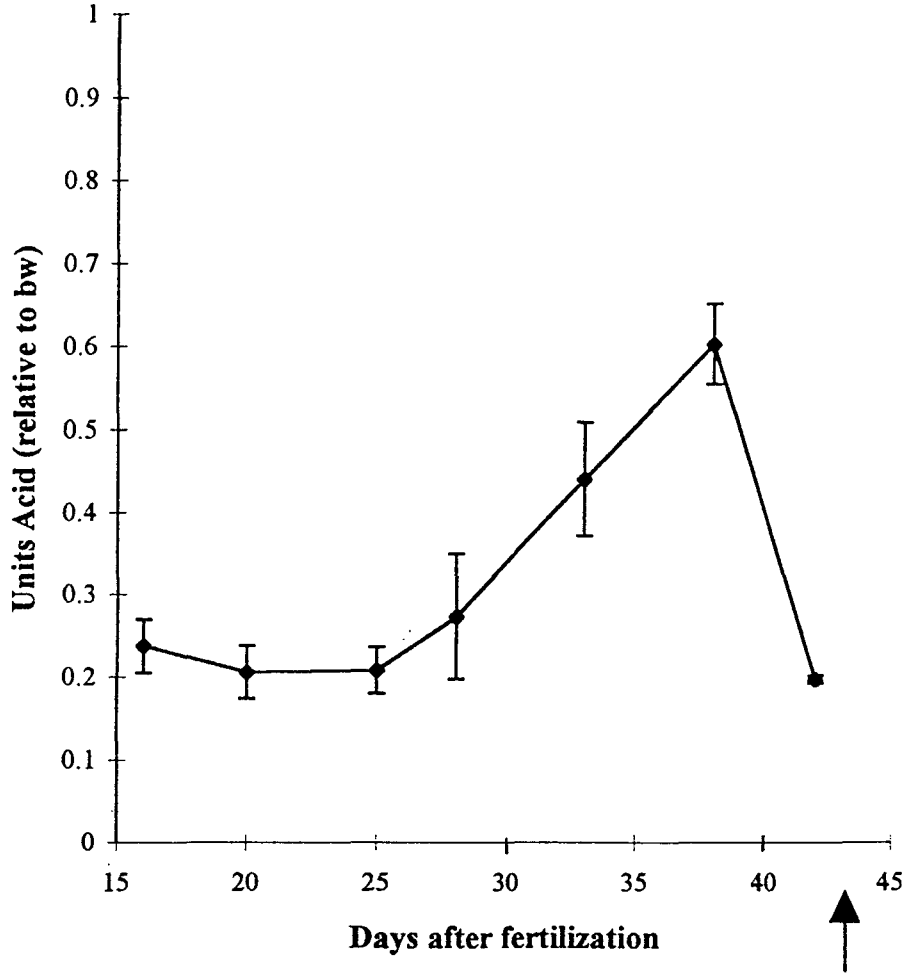
Units Acid (relative to bw)
1
0.9
0.8
0.7
0.6
0.5
0.4
0.3
0.2
0.1
0
15
20
25
30
35
40
45
Days after fertilization

Figure 3.3: Changes in acidity with respect to bath water measured at various locations around dechorionated embryos at various stages of late embryonic and early larval development. Arrow indicates day of hatching. **A.** Gills, **B.** Trunk, **C.** Yolk Sac. Bath pH was 7.9. Means ± SE, n=4-5.

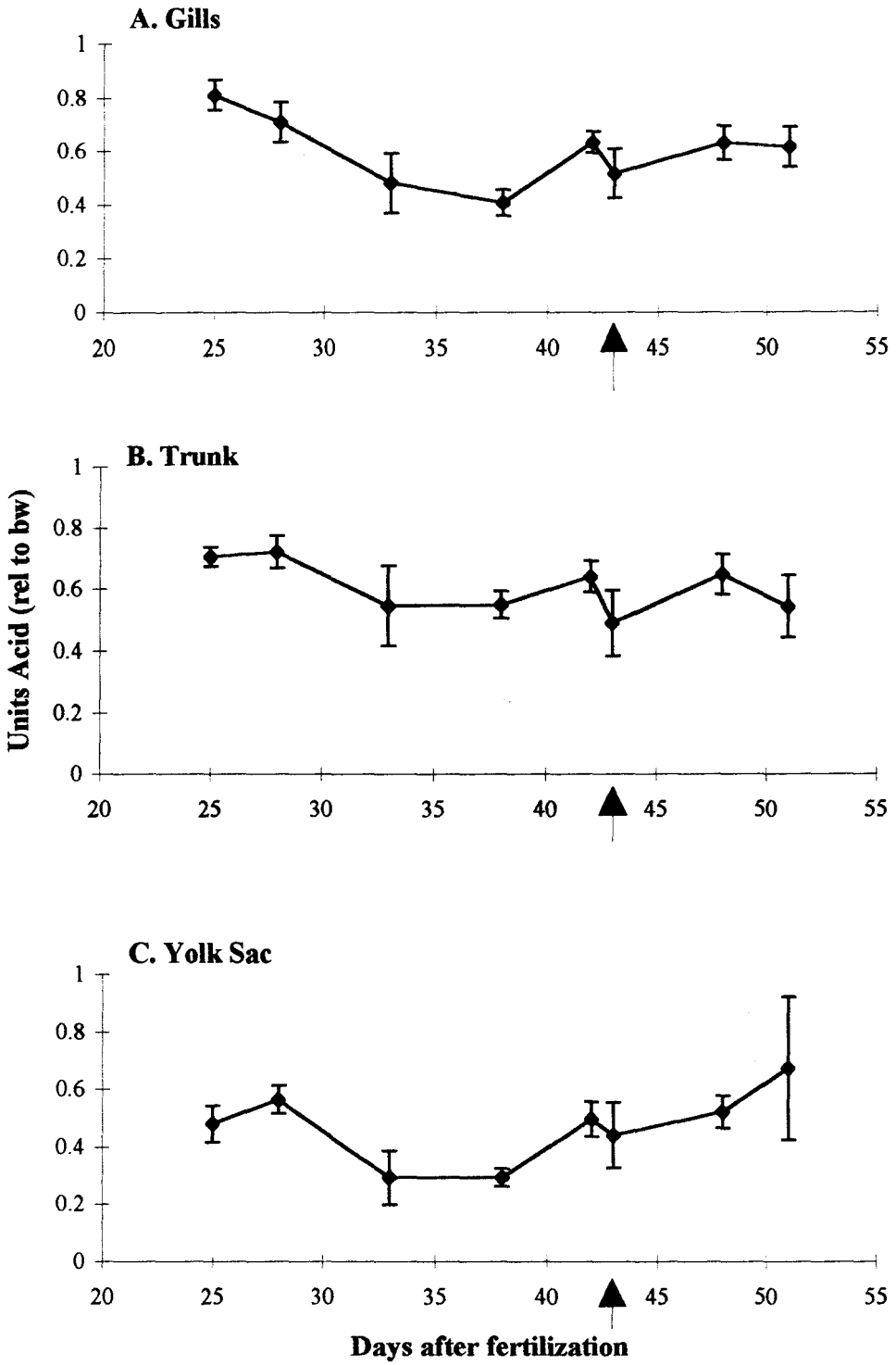
A. Gills
B. Trunk
C. Yolk Sac
Units Acid (rel to bw)
1
0.8
0.6
0.4
0.2
0
20
25
30
35
40
45
50
55
Days after fertilization

did not change dramatically between day 25 and 42 and the USL adjacent to all body surfaces did not change significantly between day 42 and 43 (day of hatching).

pH/ P_{CO2} Microelectrodes

The use of double- barrel pH/ P_{CO2} electrodes has not been previously documented in whole live animal preparations. Manufacturing the electrodes was relatively simple and approximately 60% of all electrodes made were functional. Prior to each experiment it was necessary to immerse the electrode tip for 30 minutes in a solution of bath water equilibrated with 9% CO_2 (the highest P_{CO2} standard). A single working electrode had an average lifetime of 6-8 hours. Close contact with the mucous layer around the surface of the embryo often damaged the electrode, especially if the embryo moved excessively. In addition, the short column of ionophore cocktail was easily displaced from the tip if the electrode was moved frequently between calibration solutions. Ideal column stability was acheived if electrode tips were not too long or broken and if transfer of the electrode between solutions was minimized.

Functioning electrodes were characterized by very small changes in the signal from the P_{CO2} barrel during pH changes and very small changes in the pH signal during P_{CO2} changes (Figure 3.4). It took approximately 5-10 seconds for the P_{CO2} barrel to respond to changes in CO_2 tensions and signal equilibration was acheived in 1-2 minutes. It was difficult to ensure that pH of the P_{CO2} calibration solutions was equal. As a result, the pH barrel often responded to changes in P_{CO2} because of the difference in pH between them. No correction factor was required for the P_{CO2} response in these cases because the signal

Figure 3.4: Sample chart recordings for pH/P_{CO2} microelectrode calibrations

A. pH calibration: signal from pH barrel with pH change (0.8 pH units).

B. pH calibration: signal from P_{CO2} barrel with pH change.

***C.** P_{CO2} calibration: signal from pH barrel with P_{CO2} change (2% to 9% CO_2).

***D.** P_{CO2} calibration: signal from P_{CO2} barrel with P_{CO2} change.

* It is difficult to ensure that the P_{CO2} calibration solutions have the same pH. As a result, chart recordings show a response from the pH barrel during P_{CO2} calibrations (Panel C). This does not interfere with the recordings from the P_{CO2} barrel, since the P_{CO2} signal is subtracted from the pH signal before it is recorded. Also the chart recordings show that the P_{CO2} signal is not affected by changes in solution pH (Panel B).

Signals go offscale as a result of the creation of an open circuit when electrodes are moved between solutions.

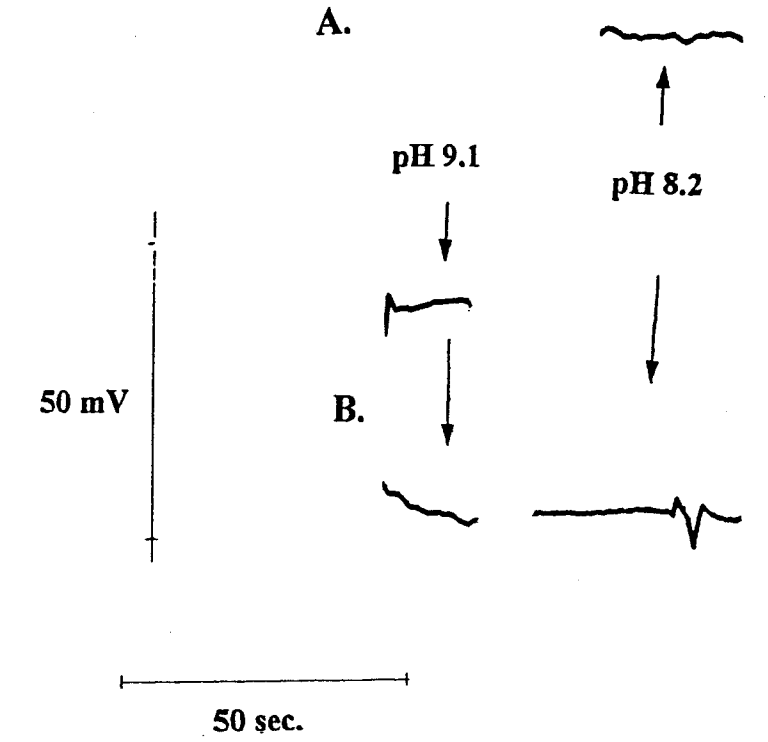
A.
pH 9.1
pH 8.2
50 mV
B.
50 sec.

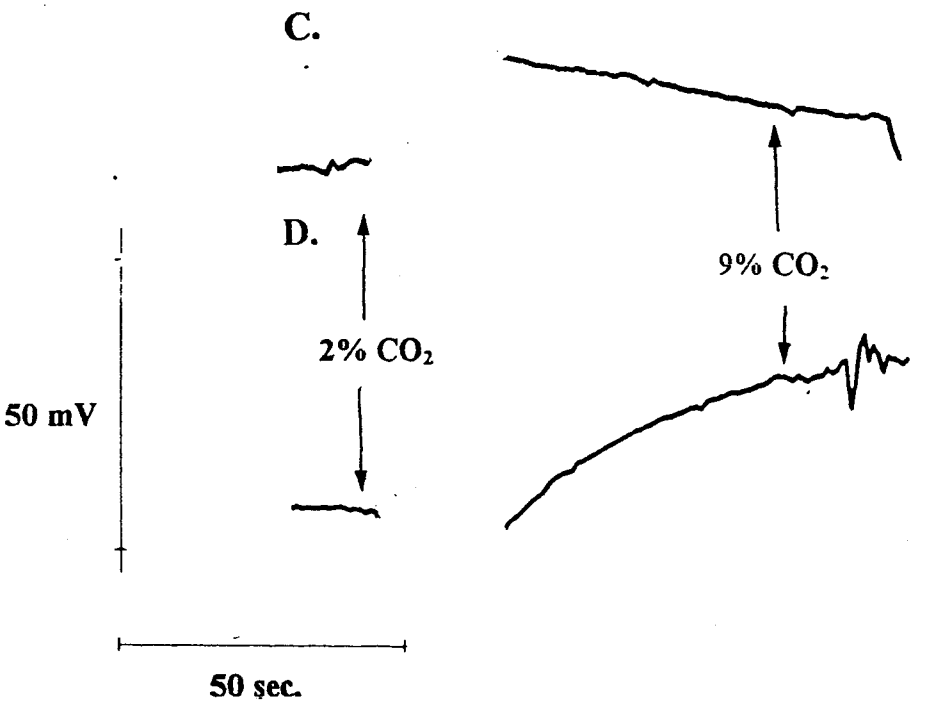
C.
D.
9% CO2
2% CO2
50 mV
50 sec.

recorded from the P_{CO2} barrel is subtracted from the pH signal. In addition, the lack of a response by the P_{CO2} barrel to changes in pH confirms that the electrode was working properly (Figure 3.4).

It is also important to notice that as electrodes were moved between calibration and experimental solutions, the electrodes were exposed to the air briefly, thus creating an open circuit. As a result, the signals went offscale.

Signals from the P_{CO2} barrel were not symmetrical; that is, electrodes were quick to respond when moved from low to high P_{CO2}, but were slow to recover when moved from the high to low P_{CO2}. It is likely that the diffusion time of CO_2 and H^+ (which trigger the electrode response) into the ionophore cocktail and backfill solution was faster than the diffusion time of these materials out of the cocktail and backfill solutions.

pH and P_{CO2} Adjacent to the Surface of Dechorionated Embryos

The USL around the gills was found to be significantly more acidic than the bath water throughout embryonic development. pH of the USL was 7.7 ± 0.1, while pH of the bath water was 8.9 ± 0.1 (n=14). The extent of USL acidification using this technique was greater than the extent of USL acidification using the pH/NH_4^+ technique because the pH of the bath water used in the latter technique was 7.9.

P_{CO2} was higher in the USL adjacent to the embryo than in the bulk water; the P_{CO2} of the USL and bulk water was 10.78 ± 2.6mmHg and 3.98 ± 0.7 respectively (n= 14). HCO_3 concentrations were calculated from the Henderson- Hasslebalch equation:

$$[HCO_3^-] = (10^{\wedge}(pH-pK))*\alpha*P_{CO_2}$$

where **$[HCO_3^-]$** was bicarbonate concentration in mmol/l; **pH** was the pH of the USL or bath water; **pK** was the equilibrium constant for conversion of CO_2 to HCO_3 at a given temperature and salinity; α was the solubility coefficient of CO_2 at a given temperature and salinity ($mmol*L^{-1}mmHg^{-1}$); P_{CO_2} was partial pressure of CO_2 in torr or mmHg. $[HCO_3^-]$ was 157.5 ± 38.4 mmol/l and 37.2 ± 7.5 mmol/l in the bulk water and the USL, respectively.

$[NH_4^+]$ Adjacent to Eggs and Dechorionated Embryos

The unstirred layer around whole eggs had a significantly higher $[NH_4^+]$ than the bulk water. The average bulk water $[NH_4^+]$ was 1.92μmol/l, while the range of egg USL $[NH_4^+]$ was 5.0 ± 1.6 to 20.2 ± 2.2μmol/l (t-test, $p<0.5$) (Figure 3.5). There was a significant increase in $[NH_4^+]$ between day 28 and 32 (from 7.2 to 21.2μmol/l) followed by a decrease between day 38 and 42 (ANOVA, $p<0.05$).

There was also a significantly higher $[NH_4^+]$ around the surface of the dechorionated embryo than in the bulk water between day 25 and 51 (t-test, $p<0.05$) (Figure 3.6). $[NH_4^+]$ ranged from 13.5 ± 3.5 to 68.0 ± 16.4μmol/l next to the gills, 11.2 ± 1.4 to 39.6 ± 5.9μmol/l next to the trunk, and 7.8 ± 4.5 to 23.7 ± 4.5μmol/l next to the yolk sac. $[NH_4^+]$ of the USL adjacent to the gills was slightly but significantly higher than

Figure 3.5: NH_4^+ concentration in the USL around whole eggs at different stages of embryonic development. Arrow indicates day of hatching. Average bulk water $[NH_4^+]$=1.9μmol/l. Means ± SE, n=4-5.

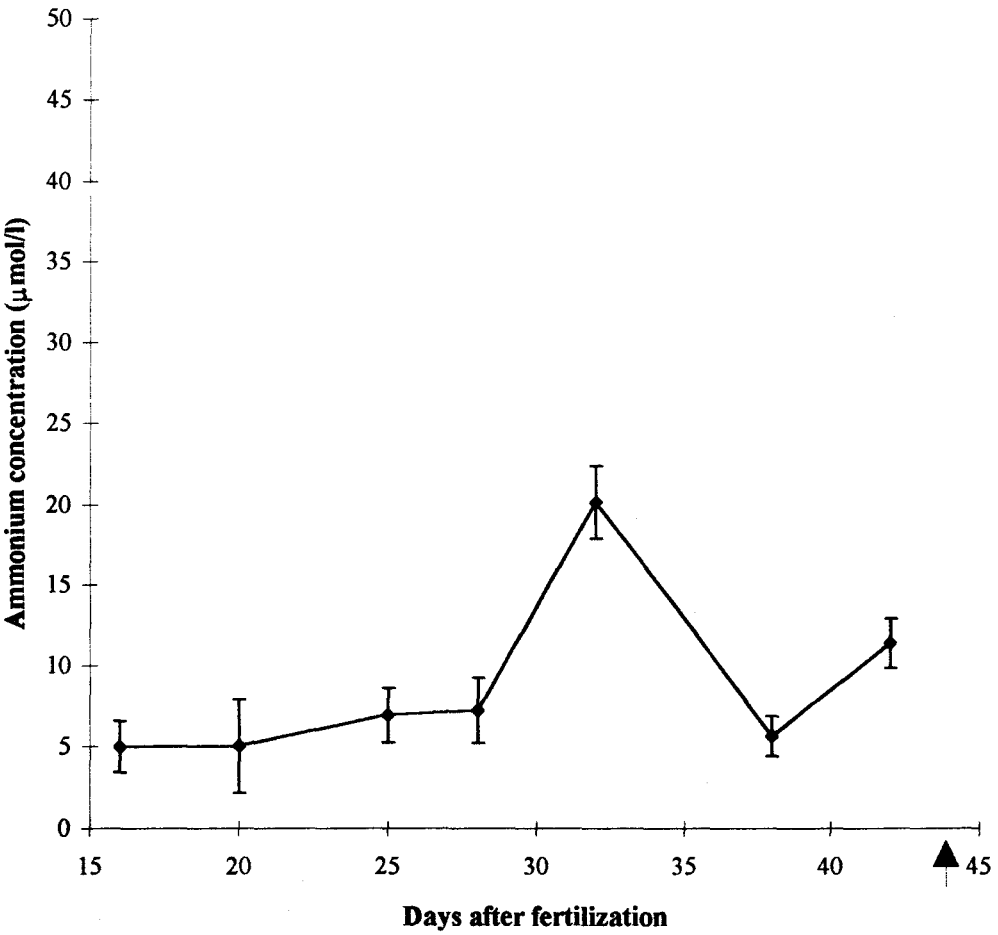
Ammonium concentration (µmol/l)
50
45
40
35
30
25
20
15
10
5
0
15
20
25
30
35
40
45
Days after fertilization

that around the trunk and was considerably higher than the USL adjacent to the yolk sac (ANOVA, $p<0.05$). There was also a significantly higher $[NH_4^+]$ around the trunk surface than around the yolk sac (ANOVA, $p<0.05$).

USL $[NH_4^+]$ adjacent to all sites changed little between day 25 and 42. At day 43 (day of hatch), there was not a significant change in $[NH_4^+]$ at any of the sites measured (ANOVA, $p<0.05$). However, $[NH_4^+]$ in the USL adjacent to the gills increased significantly from 22.2 to 59.3μmol/l between the day of hatch on day 43 and 51 (ANOVA, $p<0.05$). There were no significant differences seen in $[NH_4^+]$ around the trunk or yolk sac surfaces from day 25 to day 51 (ANOVA, $p<0.05$).

Figure 3.6: Changes in NH_4^+ concentration with respect to bulk water measured at various locations around dechorionated embryos at various stages of late embryonic and early larval development. Arrow indicates day of hatching. **A.** Gills, **B.** Trunk, **C.** Yolk Sac. Average bulk water $[NH_4^+]$= 1.9μmol/l. Means ± SE, n=4-5.

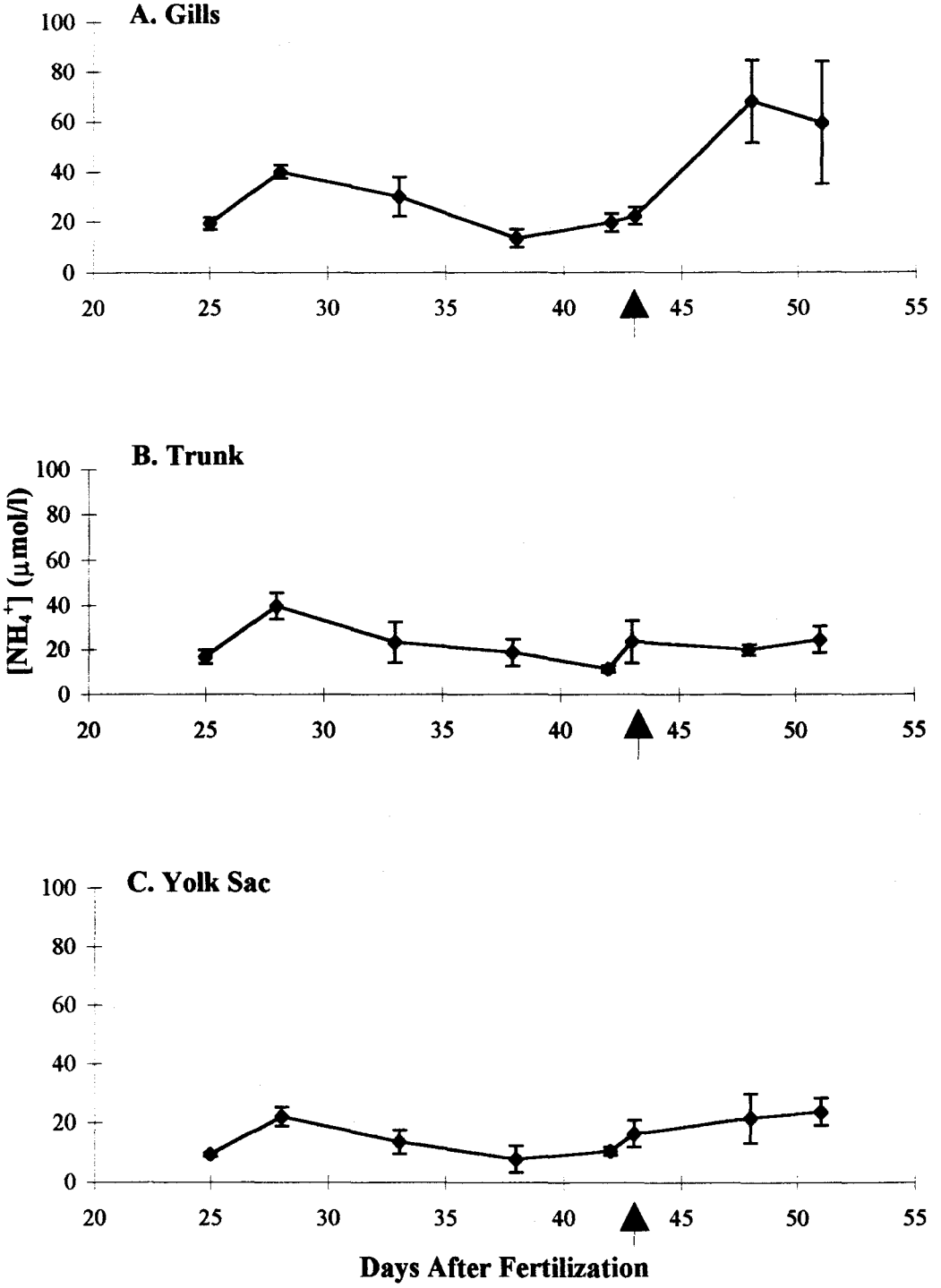
A. Gills
B. Trunk
C. Yolk Sac
100
80
60
40
20
0
20
25
30
35
40
45
50
55
[NH4+] (µmol/l)
Days After Fertilization

DISCUSSION

pH in Unstirred Layer (USL) Adjacent to Eggs and Embryos

Contributing Factors to USL acidification

The results show that whole eggs and dechorionated embryos develop an acid unstirred layer relative to the bulk water (Figure 3.2, 3.3). It is expected that since CO_2 excretion rates are considerably higher than those of NH_3 or H^+, P_{CO2} of the USL adjacent to the surface of dechorionated embryos would be the primary determinant of USL pH.

The contribution of P_{CO2} to pH of USLs can be determined by measuring the buffer capacity of the USL. However, in live embryos, buffer capacity of the USL would be quite difficult to determine, since it would require equilibrating the USL with two solutions of known P_{CO2} and measuring pH of the USL at each P_{CO2}. Exposing live embryos to gas mixtures with different P_{CO2} would drastically affect the 'normal' physiology of the animals.

Although it is likely that the buffer capacity of USLs adjacent to eggs and embryos is quite different from that of the surrounding water, a comparison of the changes in pH, P_{CO2}, and $[HCO_3^-]$ measured at the surface of dechorionated embryos, with the buffer capacity of normal water may be useful. For example, figure 3.7 compares the pH, P_{CO2}, and $[HCO_3^-]$ in the USL with the buffer capacity of typical seawater (Booth *et al.*, 1984). This comparison reveals that based on a seawater buffer capacity, approximately 40% of

Figure 3.7: A comparison of pH, P_{CO2}, and $[HCO_3^-]$ in the USL adjacent to gills of dechorionated embryos to seawater buffer curve (from Booth *et al.*, 1984). Means ± SE, n=14.

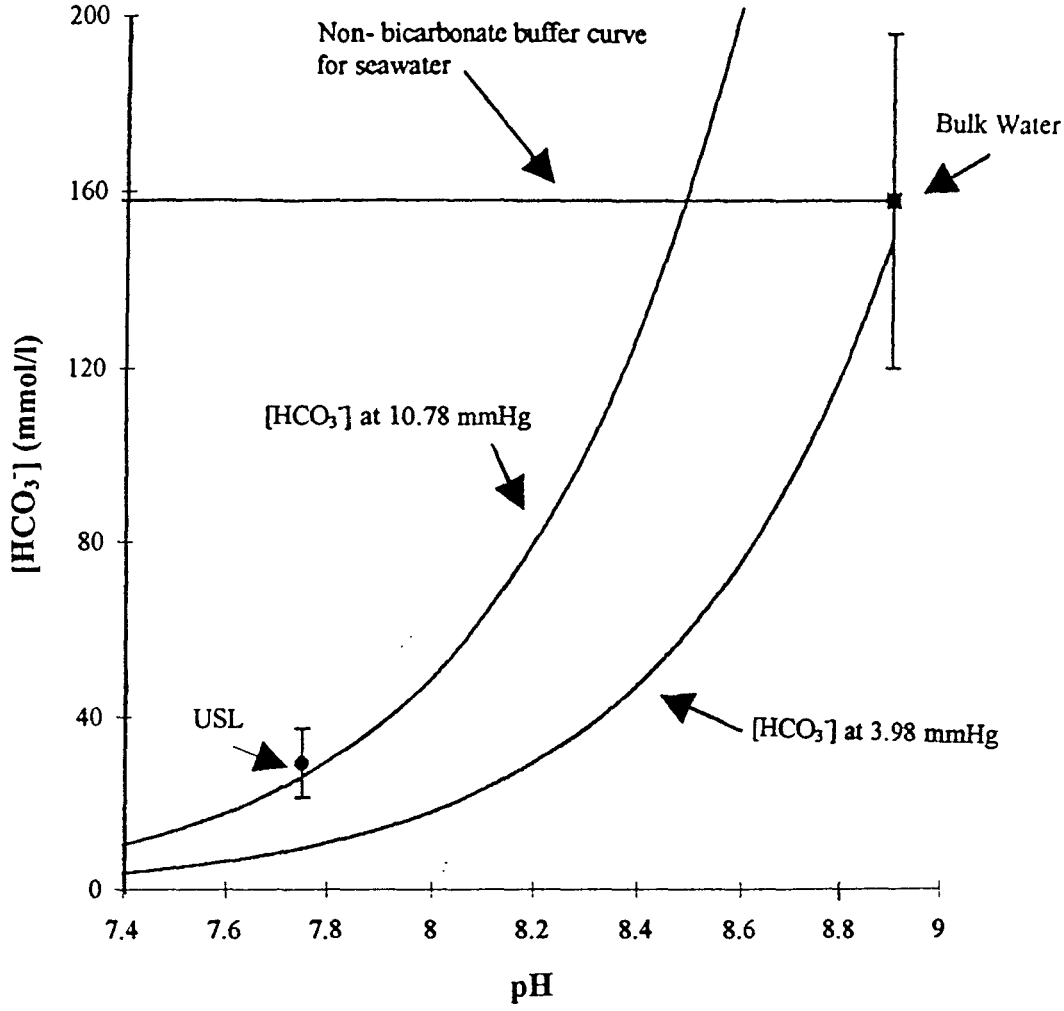
200
160
120
80
40
0
[HCO3-] (mmol/l)
Non- bicarbonate buffer curve for seawater
Bulk Water
[HCO3-] at 10.78 mmHg
USL
[HCO3-] at 3.98 mmHg
7.4
7.6
7.8
8
8.2
8.4
8.6
8.8
9
pH

USL acidification adjacent to dechorionated embryos is due to CO_2 excretion, while 60% is due to other acid sources. This is likely a great underestimation of the contribution of CO_2 to USL acidification. Since typical freshwater likely has a buffer capacity which is considerably lower than that of seawater, it is probable that CO_2 excretion contributes much more to USL acidification than this analysis suggests.

In addition, in the present experiment, bulk water was titrated to pH 8.9 for the purpose of measuring larger pH differences at the surface of embryos. It is possible that a bulk water pH of 8.9 creates a non-equilibrium situation for the embryos in which 'normal' ion and acid-base balance cannot be acheived. It is important to extend this experiment to include embryos bathed in solution of physiological pH.

Despite the problems of using bathwater with such a high pH, the results show clearly that double-barrel ISMEs for pH/P_{CO2} measurements can be a useful and important tool for determining the effect of CO_2 excretion on pH changes in unstirred layers of live animal tissue.

pH Localization

Data collected in this study between day 25 and day 51 after fertilization showed that USL acidification occurred at all sites at all days (Figure 3.2, 3.3). It is likely that USL acidification occurs prior to this, since metabolic rate and presumably CO_2 production increase rapidly after fertilization (Boulekebache, 1981). The results of the present experiment agree with those of Rahaman- Norohna *et al.*(1996) which found that an acid USL (0.32 pH units acid relative to the bulk water) exists around 40 day- old *O.*

mykiss eggs. This, they argued, was similar to the acidification found in the USL adjacent to adult rainbow trout gills.

It was found that the USL around the gills and trunk (cutaneous surface not including the yolk sac) was more acidic than the USL around the yolk sac (Figure 3.3). Assuming that CO_2 excretion contributes largely to the pH of USL, the trunk and gills must play a greater role in respiratory gas exchange than the yolk sac. Recently it has been shown that although cutaneous surfaces (body and yolk sac) contribute to greater than 70% of respiratory gas exchange prior to hatching, the yolk sac plays a minor role in whole body gas exchange in rainbow trout and Atlantic salmon (Rombough, 1998; Wells and Pinder, 1996). Wells and Pinder (1996) and Rombough (1998) argued that although the yolk sac has a large surface area and an elaborate circulatory system, it is responsible for less than 35% of total O_2 uptake. Despite the minimal contribution by the yolk sac to USL acidification, it is clear that the gills play a major role in USL acidification. This suggests that the gills are capable of functioning to some degree prior to hatching.

It is noteworthy that the USL around the chorion is less acidic than the USL adjacent to the embryo. Measurements of pH in the USL adjacent to eggs were made at a greater distance from the cellular source of CO_2 and H^+ excretion than those made at the surface of dechorionated embryos. As a result, it was expected that the concentrations of CO_2 and H^+ would be lower at the surface of the eggs. Although the dechorionated embryos were anaesthetized, it is likely that their metabolic rates were high enough to excrete significant amounts of metabolic waste products into the USL. Unanesthetized

embryos enclosed in their chorions would produce greater amounts of metabolic waste products in a given time than anaesthetized embryos, but the concentration of these products would still be higher in the USL adjacent to the embryo than in the USL adjacent to the egg.

pH Changes Through Late Embryonic and Early Larval Development

The extent of USL acidification adjacent to dechorionated embryos did not change significantly between day 25 and day 51 (Figure 3.3). Patterns of USL acidification adjacent to eggs were more pronounced than those adjacent to the embryo prior to hatching (day 43). Again, these differences may be attributed partly to the use of anaesthesia in dechorionated embryos. These embryos moved and ventilated much less than the embryos within their chorions. Given that USL acidification is due primarily to CO_2 excretion, an inhibition of ventilation and activity would likely result in less dramatic changes in pH of the USL around the dechorionated embryos. Also, pH measurements were made only at 3 sites around embryos. It is possible that if measurements were made at more sites, the dramatic changes in pH adjacent to the whole egg would be accounted for at the surface of the embryo. The changes that occur at the surface of the egg may be an average or sum of the changes occurring at all sites adjacent to the embryo. Finally,inherent variability between animals sampled may have contributed to the lack of similarity in pH patterns in the USL adjacent to whole eggs and dechorionated embryos.

The data from dechorionated embryos and first day hatchlings from the present investigation can be compared to those found previously in rainbow trout hatchlings

(Misiaszek, 1996). In recent hatchlings, Misiaszek (1996) determined that pH at the surface of the gills, trunk, and yolk sac was acid relative to the bulk water. The same study also showed a large peak in acidity at the surface of first- day hatchlings. This peak, Misiaszek (1996) argued, was due to a transient increase in metabolic oxygen consumption resulting from the repayment of an oxygen debt associated with hatching. The present experiment did not show a similar peak in acidity. It is not likely that O_2 supplies are limited to the developing embryos within hours or days of hatching, since O_2 permeability of the chorion is relatively high (Peterson and Martin-Robichaud, 1986). In addition, small holes can be seen within the chorion a few days prior to hatching, probably as a result of the activity of the hatching enzyme. This would further break down any O_2 diffusion barriers across the chorion.

$[NH_4^+]$ in USL of Eggs and Dechorionated Embryos

Contributing Factors to $[NH_4^+]$ in USL

At least 3 factors will influence $[NH_4^+]$ in USL adjacent to eggs and embryos. Firstly, protein catabolism from the yolk sac is the major source of energy for developing teleost embryos (Kamler, 1992). As a result, NH_3 production is likely to occur in eggs at a very early age (Kamler, 1992). Since NH_3 is very toxic to organisms, eggs and embryos must possess an ability to excrete it into the pvf, environment, or both (Wright, 1995; Rahaman- Norohna *et al.*, 1996). NH_3 production and excretion may vary within eggs (i.e. different sites of embryos may produce and excrete NH_3 more than others).

Secondly, pH of the USL adjacent to organisms will affect the amount of NH_3 excreted and the amount of NH_3 that will be converted to NH_4^+. The conversion of NH_3 to NH_4^+ has a pK of 9.5 (Randall and Wright, 1989; Wright, 1995; Rahaman-Norohna *et al.*, 1996). As a result, most of the NH_3 excreted from typical rainbow trout tissues into typical freshwater will be converted to NH_4^+ in the USL, since most tissues and freshwater have a pH less than 9.5. P_{NH3} will tend to be higher in more alkaline tissue 'compartments' and NH_3 will tend to diffuse into more acidic compartments such as the yolk or pvf (Rahaman- Norohna *et al.*, 1996). The conversion of NH_3 to NH_4^+ in the USL maintains a P_{NH3} gradient favouring NH_3 excretion.

Finally, permeability of body and egg tissues to NH_3 or NH_4^+ will affect $[NH_4^+]$ in the USL. Although it has been suggested that NH_4^+ electrochemical gradients play a role in ammonia transfer across cell membranes, the extent of NH_4^+ permeability across embryonic and chorionic tissues is unclear (Rahaman- Norohna *et al.*, 1996; Wright *et al.*, 1988). Nonetheless, two sites with similar USL pH may have different $[NH_4^+]$ by virtue of different permeabilities to NH_3 or NH_4^+.

Localization of $[NH_4^+]$ in USL

The results of this investigation showed that USL of eggs and dechorionated embryos had a relatively high concentration of NH_4^+ compared to the bath water (Figure 3.5, 3.6), suggesting an ability of embryos to excrete considerable quantities of NH_3 prior to hatching. It is important to point out that this investigation did not include the measurement of NH_3 excretion rates. Determining excretion rates would have required

the measurement of 2 concentrations of NH_4^+ at 2 locations away from the eggs and embryos (based on Fick's Law). However, in the present study only single point measurements were made and no flux calculations were performed. Nonetheless, this method provides a qualitative indication of the extent of NH_3 excretion (by measuring NH_4^+ concentration) throughout the end of embryonic and the start of larval development, assuming constant USL pH on each sampling day. It also provides evidence for the ability of NH_3 and/or NH_4^+ to cross the chorion.

The USL around whole eggs was shown to have a low [NH_4^+] relative to the surfaces of dechorionated embryos. Since measurements made at the USL adjacent to the chorion were further away from the source of NH_3 excretion than those made at the USL adjacent to the embryo, a lower [NH_4^+] may have been expected. Whether embryos were anaesthetized or not, it was expected that a constant production and excretion of NH_3 and/or NH_4^+ by embryos would result in a higher concentration of the molecule in the USL adjacent to the source of excretion than in the USL adjacent to the chorion. It is also possible that as NH_3 is excreted from the animal it combines with H^+ in the pvf (an acid compartment) and gets 'trapped' as NH_4^+, a relatively impermeable molecule (Rahaman-Norohna *et al.*, 1996; Wright *et al.*, 1988). This would aid in the explanation of the low [NH_4^+] measured in the egg USL.

The results showed only a slightly higher concentration of NH_4^+ in the USL near the gills than in the USL near the trunk, relative to bath water prior to hatching (Figure 3.6). This provides further evidence for the importance of cutaneous surfaces in metabolic

gas exchange in embryonic teleosts. In larval and adult rainbow trout, it has been shown that the gills are the predominant source of ammonia excretion (Misiaszek, 1996; Wright, 1995; Wright *et al.* 1995).

The USL adjacent to the yolk sac had a NH_4^+ concentration that was less than half that found around the gills and trunk. Since the yolk sac contains a very high NH_4^+ concentration (3000μmol/L) it was expected that the P_{NH4+} gradient would be favourable for NH_4^+ excretion (Rahaman- Norohna *et al.*, 1996). The relatively low $[NH_4^+]$ measured adjacent to the yolk sac reflects the impermeability of the yolk sac to NH_4^+. As NH_3 is excreted from the body into the yolk sac, which has been shown to be an acid compartment, it combines with H^+ to form NH_4^+. NH_4^+ is a relatively large molecule and it gets 'trapped' in the yolk sac (Rahaman- Norohna *et al.*, 1996).

$[NH_4^+]$ Changes Through Late Embryonic and Early Larval Development

Despite the similarity between gills and trunk prior to hatching (between day 25 and 42), there was a significant increase in $[NH_4^+]$ adjacent to the gills immediately after hatching (after day 43) (Figure 3.6). These changes in NH_4^+ were not accompanied by changes in pH. In addition, changes in $[NH_4^+]$ that occurred adjacent to gills were not accompanied by changes at the trunk or yolk sac. This suggests that the permeability of gill tissue to NH_3 and/or NH_4^+ increases after hatching. It has been shown that O_2 permeability of yolk sac and trunk surfaces decreases steadily as yolk sac absorption occurs, since the skin on these surfaces thickens after hatching (Rombough, 1998; Wells

and Pinder, 1996a,b). This likely influences permeability of the yolk sac and trunk to other materials such as NH_3 and NH_4^+, and possibly affects gill permeability.

These results agree with those of Misiaszek (1996), which determined that although $[NH_4^+]$ adjacent to the gills increased dramatically after hatching, $[NH_4^+]$ adjacent to other body surfaces did not change after hatching. The change in $[NH_4^+]$ adjacent to the gills may be associated with the development and elaboration of gill tissue which may allow for an increase in NH_3/NH_4^+ permeability (Misiaskek, 1996; Morgan, 1974).

From day 28 to hatching, there seemed to be no dramatic changes in $[NH_4^+]$ adjacent to the embryo (Figure 3.6). This is consistent with the finding that NH_3 excretion rates do not change significantly in rainbow trout embryos over this same period (Wright *et al.*, 1995). Since protein catabolism is the primary source of energy for developing embryos (Kamler, 1992), the lack of a change in either $[NH_4^+]$ or NH_3 excretion rate by the embryo within 2 weeks of hatching suggests that metabolic rate remains relatively constant during this period (Wright *et al.*, 1995). Rombough (1988) argued that changes in metabolic rate during embryonic development are not clear; some studies show a large change, while others show a small, gradual change. Still others suggest that there may be a slight decline in metabolic rate prior to hatching (Rombough, 1988).

Conclusions

- USL acidification occurs adjacent to whole eggs and dechorionated embryos.

- P_{CO2} is higher in the USL adjacent to the gills than in the bulk water and likely accounts for most of the USL acidification.

- Gills and trunk contribute more to USL acidification than yolk sac, pointing to the importance of these surfaces prior to hatching.

- Gills are the primary site of NH_3/NH_4^+ excretion prior to hatching. There is likely an increase in gill permeability to these molecules as the gills develop after hatching.

- Low concentrations of NH_4^+ in the USL adjacent to yolk sac and chorion suggest a role of 'acid trapping' in NH_3 and/or NH_4^+ excretion across the yolk sac and pvf.

CHAPTER 4: GENERAL DISCUSSION

Ion Balance

This study has demonstrated influxes, effluxes, and redistribution of ions by eggs and embryos of rainbow trout prior to hatching. Accumulation of the major cations and anions, Ca^{2+}, Na^{+}, and Cl^{-}, by whole eggs and embryos suggests that embryos posses the required mechanisms for ion regulation and possibly for ion uptake from the environment. Although exchange of Ca^{2+}, Cl^{-}, and Na^{+} is believed to occur across mitochondria rich cells in the yolk sac, trunk, pericardial region and primary gill lamellae (Li *et* al., 1995; Ayson *et* al., 1994; Hwang *et* al., 1994; Alderdice, 1988; Hwang and Hirano, 1985), there is a lack of quantitative evidence for this in the literature. Because of the differences in Na^{+} and Ca^{2+} by dechorionated embryos (Table 2.4, 2.5) and developing larvae (Misiaszek, 1996), it is possible that the mechanism for Na^{+} regulation is different from that for Ca^{2+} regulation and that these mechanisms develop at different stages of development.

The results also suggest that not all body surfaces contribute equally to ion regulation prior to hatching. Developing embryos and larvae may take these ions up from different locations (i.e. Na^{+} may be taken up primarily from pvf or environment, while Ca^{2+} may be taken up primarily from the yolk sac) and some tissues may contribute more than others to ion regulation (i.e. gills, body, yolk sac).

A profitable area for future research will be the analysis of sites and mechanisms of Ca^{2+}, H^+, Na^+ and Cl^- fluxes in isolated embryos (Somieski and Nagel, 1998; Smith *et al.*, 1994; Kuhtreiber and Jaffe, 1990). The self-referencing ion probe and the vibrating current density probe techniques are useful because they have very low noise and resolve very small signals (i.e. self-referencing ISMEs can resolve μV changes whereas static ISMEs can resolve only mV changes). Whereas the vibrating current density probe measures the current produced by ion fluxes in the USL adjacent to cells, the self-referencing ion selective probe measures the activity of specific ions (Somieski and Nagel, 1998; Smith *et al.*, 1994). Recently, the former technique has been used to show that Cl^- movement across frog epithelia is via paracellular pathways between MRCs (Somieski and Nagel, 1998). Both techniques may be of great use in determining the extent and mechanisms of ion fluxes in embryonic teleost tissues. For example, the role of MRCs in the exchange of ions across the yolk sac, branchial, and cutaneous surfaces can be investigated using these techniques.

Metabolic Gas Exchange and USL Acidification

This study has also shown that sites of exchange of H^+, NH_4^+, and CO_2 can be determined by ISME analysis of the USL of developing eggs and embryos. This non-invasive technique has a fine spatial resolution (<100μm). This technique has shown that not all body surfaces contribute equally to metabolic gas exchange and waste excretion. The gills are a predominant site of CO_2 and NH_3/NH_4^+ exchange. The trunk surface also

plays an important role in the exchange of these materials, whereas the yolk sac plays a minor role. This suggests that although the gills are not fully developed until hatching, they are clearly capable of ion and gas exchange prior to hatching. It also provides further evidence for the role of cutaneous surfaces in embryonic and larval respiration and metabolism. Investigating the possibility of changes in permeability of gills, trunk, and yolk sac surfaces to NH_3, NH_4^+, and other ions, due to thickening of skin after the 'eyed' stage would be useful.

Furthermore, it is important to determine the specific location of NH_3/NH_4^+ production and the extent and mechanism of NH_4^+ excretion in embryonic rainbow trout. Although it is believed that NH_4^+ is relatively impermeable across yolk sac epithelia (Rahaman-Norohna *et al.*, 1996), there have been few, if any, studies measuring the permeability of gill and trunk surfaces to NH_4^+.

Acidification of USL was determined to be significant at all ages and locations measured adjacent to eggs and dechorionated embryos. This, and the fact that significant concentrations of NH_4^+ were measured at the surface of eggs and embryos, suggests that embryos are capable of catabolizing proteins from the yolk sac and producing CO_2 via aerobic metabolism.

It is not known whether sites of CO_2 and NH_3/NH_4^+ excretion correspond to sites of ion exchange and whether these processes are linked. Rahaman-Norohna *et al.* (1996) found that increasing external [Na^+] resulted in increased NH_3 excretion rates but that exposure to low external [Na^+] had no effect on ammonia excretion rates. They have also found that a low pH corresponds to high NH_3 excretion rate by virtue of a large P_{NH3}

gradient across the body and egg surfaces. It is possible that changes in external ion concentrations (Na^+, Ca^{2+}, and Cl^-) have an effect on external pH by interfering with H^+ exchange across embryonic epithelia, which in turn affects NH_3 excretion.

The present study compliments recent work by Rombough (1998) on the localization of P_{O2} in embryonic teleosts, Misiaszek (1996) on the development of ion regulation in larval rainbow trout, and Rahaman-Norohna *et al.* (1996) on the localization of H^+ (CO_2) and NH_4^+ excretion in rainbow trout eggs. All of these studies have shown that measuring concentrations and fluxes of materials at the surface of eggs, embryos, and larvae provides useful information on the development of various body tissues and processes. Methods such as those used in this study can potentially be used to study transcutaneous fluxes and concentrations of any substance consumed or excreted across embryonic and larval teleost surfaces.

Advantages of Dechorionating Embryos

Techniques for the dechorionation of embryos are relatively simple and were invaluable for most of the experiments in this study. It was found that embryos removed from their chorions were viable; dechorionated embryos survived in excess of 2 weeks in small volumes of saline or dechlorinated tap water at 4°C. This observation raises questions concerning the functional significance of the pvf and chorion. Although research on chorions has revealed information on permeability characteristics (Peterson and Martin-Robichaud, 1993, 1986), it is not known how important the chorion and pvf are for ion regulation, acid-base balance and long-term survival of embryos. It is possible

that although the pvf and chorion provide protection from mechanical damage during embryonic development, these compartments are not essential for maintaining ionic and acid-base homeostasis after the 'eyed' stage.

Although it may be argued that removing the chorion from embryos early in development creates an artificial situation for the embryos, dechorionating embryos provides direct access to the developing tissues. For example, dechorionation of embryos allows direct access to developing gills, and questions pertaining to gill structure prior to hatching can be addressed using TEM and SEM techniques. In addition, removal of the chorion from embryos will allow for the study of cardiac function, blood gas composition, tissue enzyme activity, and aerobic capacity in embryos. Use of dechorionated embryos will permit a more direct investigation of the effects of pollutants such as cadmium, copper, zinc, and silver, on ion regulation, metabolism and development in early life stages. In addition, techniques such as patch clamping and ion probe analysis can be applied directly to the live tissues of dechorionated embryos and will provide a clearer indication of the ability of embryos to establish and maintain ionic homeostasis.

REFERENCES

Alderdice, D.F. 1988. Osmotic and ionic regulation in teleost eggs and larvae *In* Fish Physiology (ed. W.S. Hoar and D.J. Randall), Vol XIA, p. 163-251. Academic Press, New York.

Ammann, D. 1986. Ion-selective microelectrodes. Spinger-Verleg, Berlin.

Ayson, F.G., T. Kanenko, S. Hasegawa. 1994. Development of mitochondrion-rich cells in the yolk sac membrane of embryos and larvae of Tilapia, Oreochromis mossambicus, in freshwater and seawater. *J. Exp. Zool.* 270: 129-135.

Baxter, J.H.S. 1969. Development: Eggs and Larvae. *In* Fish Physiology Vol. 3 (Eds. W.S. Hoar and D.J. Randall). p. 177-252. Academic Press, Inc., New York.

Booth, C.E., D.G. McDonald, P.J. Walsh. 1984. Acid-base balance in the sea mussel, *Mytilus edulis*. I. Effects of hypoxia and air-exposure on hemolymph acid-base status. *Marine Biology Letters*. 5: 347-358.

Boulekebache, H. 1981. Energy metabolism in fish development. *Amer. Zool.* 21: 377-389.

Collier, K.A., M.J. O'Donnell. 1997. Analysis of epithelial transport of K^+, Cl^-, and pH gradients in extracellular unstirred layers: Ion secretion and reabsorption by Malpighiam tubules of *Rhodnius proxilus*. *J. Exp. Biol.* 200: 1627-1638.

Eddy, F.B. 1982. Osmotic and ionic regulation in captive fish with particular reference to salmonids. *Comp. Biochem. Physiol.* 73B(1): 125-141.

Eddy, F.B. 1974. Osmotic properties of the perivitelline fluid and some properties of the chorion of Atlantic salmon eggs (Salmo salar). *Can. J. Zool.* 174: 237-243.

Eddy, F.B., C. Talbot. 1985. Sodium balance in eggs and dechorionated embryos of the atlantic salmon Salmo salar L. exposed to zinc, aluminum and acid waters. *J. Comp. Biochem. Physiol.* 81C (2): 259-266.

Heming, T.A., R.K. Buddington. 1988. Yolk absorption in embryonic and larval fishes. *In* Fish Physiology. Vol XIA. Eds: W.S. Hoar and D.J. Randall. Academic Press Inc., New York. pp 407-446.

Hwang, P.P. 1989. Distribution of chloride cells in teleost larvae. *J. Morph.* 200: 1-8.

Hwang, P.P., R. Hirano. 1985. Effects of environmental salinity on intercellular organization and junctional structure of chloride cells in early life stages of teleost development. *J. Exp. Zool.* 236: 115-126.

Hwang, P.P., Y.N. Tsai, Y.C. Tung. 1994. Calcium balance in embryos and larvae of the freshwater-adapted teleost, Oreochromis mossambicus. *Fish Physiol. Biochem.* 13(4): 325-333.

Kamler, E. 1992. Early life history of fish: An energetics approach. Chapman and Hall, New York.

Karnaky, K.J. 1986. Structure and function of the chloride cell of Fundulus heteroclitus and other teleosts. *Amer. Zool.* 26: 209-224.

Kuhtreiber, W.M., L.F. Jaffe. 1990. Detection of extracellular calcium gradients with a calcium-specific vibrating electrode. *J. Cell Biol.* 110: 1565-1573.

Li, J., J. Eyegensteyn, R.A. Lock, P.M. Verbost, A.J.H. VanDer Heijden, S.E. Wendelaar Bonga, G. Flik. 1995. Branchial chloride cells in larvae and juvenilles of freshwater tilapia, Oreochromis mossambicus. *J. Exp. Biol.* 198: 2177-2184.

McDonald, D.G., B.R. McMahon. 1977. Respiratory development in Arctic char Salvelinus alpinus under conditions of normoxia and chronic hypoxia. *Can. J. Zool.* 55: 1461-1467.

McWilliams, P.G. 1993. Environment induction of Na^+ transporter affinity in Atlantic salmon embryos. *J. Fish Biol.* 42: 119-130.

McWilliams, P.G., K.L. Shephard. 1991. Water quality during egg incubation influences yolk-sac fry sodium uptake kinetics in Atlantic salmon, Salmo salar L.: a possible mechanism of adaptation to acid waters. *J. Fish Biol.* 39: 469-483.

McWilliams, P.G., K.L. Shephard. 1989. Kinetic characteristics of the sodium uptake mechanism during the development of embryos and fry of Atlantic salmon, Salmo salar L., in an improved water quality. *J. Fish Biol.* 35: 855-868.

Misiaszek, C.M. 1996. Development of ion regulation in larval rainbow trout (*Oncorhynchus mykiss*). M.Sc Thesis. McMaster University.

Morgan, M. 1974. The development of gill arches and gill blood vessels of the rainbow trout, *Salmo gairdneri*. *J. Morph.* 142: 351-364.

O'Donnell, M.J. 1992. A simple method for construction of flexible, subminiature ion-selective electrodes. *J. Exp. Biol.* 162: 353-359.

Perry, S.F., C.M. Wood. 1985. Kinetics of branchial calcium uptake in the rainbow trout: effects of acclimation to various external calcium levels. *J. Exp. Biol.* 116: 411-433.

Peterson, R.H., D.J. Martin-Robichaud. 1993. Rates of ionic diffusion across the egg chorion of Atlantic Salmon (Salmo salar). *Physiol. Zool.* 66(3): 289-306.

Pinder A.W., M.E. Feder. 1990. Effect of boundary layers on cutaneous gas exchange. *J. Exp. Biol.* 143: 67-80.

Potts, W.T.W., P.P. Rudy, Jr. 1969. Water balance in the eggs of the Atlantic Salmon Salmo salar. *J. Exp. Biol.* 50: 223-237.

Rahaman- Norohna, E., M.J. O'Donnell, C.M. Pilley, P.A. Wright. 1996. Excretion and distribution of ammonia and the influence of boundary layer acidification in embryonic rainbow trout (Oncorhynchus mykiss). *J Exp. Biol.* 199: 2713-2723.

Randall, D.J., P.A Wright. 1989. The interaction between carbon dioxide and ammonia excretion and water pH in fish. *Can. J. Zool.* 67: 2936-2942.

Randall, D.J., P.A. Wright. 1987. Ammonia distribution and excretion in fish. *Fish Physiol. Biochem.* 3(3): 107-120.

Rombough, P.J. 1998. Partitioning of oxygen uptake between the gills and skin in fish larvae: A novel method for estimating cutaneous oxygen uptake. *J. Exp. Biol.* 201-1763-1769.

Rombough, P.J. 1988. Respiratory gas exchange, aerobic metabolism, and effects of hypoxia during early life stages. *In* Fish Physiology Vol XIA. (Eds: W.S. Hoar and D.J. Randall) pp. 59-161.

Rombough, P.J. 1988. Growth, aerobic metabolism, and dissolved oxygen requirements of embryos and alevins of steelhead, Salmo gairdneri. *Can. J. Zool.* 66: 651-660.

Rombough, P.J. 1984. Disturbed ion balance in alevins of Atlantic salmon, *Salmo salar*, chronically exposed to sublethal concentrations of cadmium. *Can. J. Zool.* 62: 1443-1450.

Rombough, P.J., D. Ure. 1991. Partitioning of oxygen uptake between cutaneous and branchial surfaces in larval and young juvenile chinook salmon Oncorhynchus tshawytscha. *Physiol. Zool.* 64(3): 717-727.

Rudy, P.P., W.T.W. Potts. 1969. Sodium balance in the eggs of the Atlantic salmon, Salmo salar. *J. Exp. Biol.* 50: 239-246.

Schmidt-Neilsen, K., 1994. Animal physiology: adaptation and environment. Cambridge University Press, New York.

Shen, A.C.Y., J. F. Leatherland. 1978. Effect of ambient salinity on ionic and osmotic regulation of eggs, larvae, and alevins of rainbow trout (Salmo gairdneri). *Can. J. Zool.* 56: 571-577.

Shen, A.C.Y., J.F. Leatherland. 1978. Structure of the yolksac epithelium and gills in the early developmental stages of rainbow trout (Salmo gairdneri) maintained in different ambient salinities. *Env. Biol. Fish.* 3(4): 345-354.

Shephard, K.L. 1989. An analysis of the ion-exchange characteristics of fish-egg chorions. *Fish Physiol. Biochem.* 6(6): 395-401.

Shephard, K.L. 1987. The influence of water pH on the perivitelline fluid of perch (Perca fluviatilis) eggs. *Comp. Biochem. Physiol.* 86C (2): 383-386.

Shephard, K.L. 1987. Ion-exchange phenomena regulate the environment of embryos in the eggs of freshwater fish. *Comp. Biochem. Physiol.* 88A(4): 659-662.

Shephard, K.L., P.G. McWilliams. 1989. Ionic regulation by the eggs of salmon. *J. Comp. Physiol. B.* 159: 249-254.

Smith, P.J., R.H. Sanger, L.F. Jaffe. 1994. The vibrating Ca^{2+} electrode: a new technique for detecting plasma membrane regions of Ca^{2+} influx and efflux. *In* Methods in Cell Biology, Vol. 40, p. 115-134. Academic Press, New York.

Somieski, P., W. Nagel. 1998. Localizing transepithelial conductive pathways using a vibrating voltage probe. *J. Exp. Biol.* 201: 2489-2495.

Steingraeber, M.T., W.H. Gingerich. 1990. Hatching, growth, ion accumulation, and skeletal ossification of brook trout (Salvelinus fontinalis) alevins in acidic soft waters. *Can. J. Zool.* 69: 2266-2276.

Voipio, J., K. Ballanyi. 1997. Interstitial P_{CO2} and pH, and their role as chemostimulants in the isolated respiratory network of neonatal rats. *J. Physiol.* 499(2): 527-542.

Voipio, J., K. Kaila. 1993. Interstitial P_{CO2} and pH in rat hippocampal slices measured by means of a novel fast CO_2/H^+-sensitive microelectrode based on a PVC-gelled membrane. *Pflugers Arch.* 423:193-201.

Wells, P.R., A.W. Pinder. 1996. The respiratory development of Atlantic salmon I. Morphometry of gills, yolk sac and body surface. *J. Exp. Biol.* 199: 2725-2736.

Wells, P.R., A.W. Pinder. 1996. The respiratory development of Atlantic salmon II. Partitioning of oxygen uptake among gills, yolk sac, and body surfaces. *J. Exp. Biol.* 199: 2736-2744.

Wilson, R.W., P.M. Wright, S. Munger, C.M. Wood. 1994. Ammonia excretion in freshwater rainbow trout (Oncorhynchus mykiss) and the importance of gill boundary layer acidification: lack of evidence for Na/NH4 exchange. *J. Exp. Biol.* 191: 37-58.

Wright, P.A. 1995. Review- Nitrogen excretion: Three end products, many physiological roles. *J. Exp. Biol.* 198: 273-281.

Wright, P.A., A. Felskie, P.M. Anderson. 1995. Induction of ornithine-urea cycle enzymes and nitrogen metabolism and excretion in rainbow trout (*Oncorhynchus mykiss*) during early life stages. *J Exp. Biol.* 198: 127-135.

Wright, P.A., D.J. Randall, C.M. Wood. 1988. The distribution of ammonia and H^+ between tissue compartments in lemon sole (*Parophrysa vetulus*) at rest, during hypercapnia and following exercise. *J. Exp. Biol.* 136: 149-175.

Wright, P.A., C.M. Wood. 1985. An analysis of branchial ammonia excretion in the freshwater rainbow trout: Effects of environmental pH change and sodium uptake blockade. *J. Exp. Biol.* 114: 329-353.

Zadunaiski, J.A. 1984. 'The chloride cell': The active transport of Cl^- and the paracellular pathways. *In* Fish Physiology Vol. 10, Pt. B. (ed. W.S. Hoar and D.J. Randall). p. 129-176. Academic Press, New York.